GAMMA-RAY SPECTROSCOPY

BY

YOHANNES TEFFERA

SUBMITTED IN PARTIAL FULFILLMENT OF THE
REQUIREMENTS FOR THE DEGREE OF
MASTER OF SCIENCE IN PHYSICS
AT
ADDIS ABABA UNIVERSITY
ADDIS ABABA, ETHIOPIA
AUGUST 2018

ADDIS ABABA UNIVERSITY
DEPARTMENT OF PHYSICS
Advisor:
Dr. Tilahun Tesfaye
ADDIS ABABA UNIVERSITY
Date: AUGUST 2O18
Author: YOHANNES TEFFERA
Project Title: GAMMA-RAY SPECTROSCOPY
Department: Physics
Degree: M.Sc. Convocation: AUGUST Year: 2018

Permission is herewith granted to Addis Ababa University to circulate and to have copied for non-commercial purposes, at its discretion, the above title upon the request of individuals or institutions.

---Signature of Author

Approved by the Examination Committee

1. Advisor ________________________________
Dr. Tilahun Tesfaye

2. Examiner: ________________________________
Dr. Remudin Reshid

3. Examiner**:** ________________________________
Dr. Chernet Amente

Dated: AUGUST 2018

Contents

ACKNOWLEDGEMENTS vi
ABBREVIATIONS vii
ABSTRACT viii
Chapter 1 1
Introduction 1
1.1 Origin of gamma rays 2
1.1.1 Gamma-rays and electromagnetic spectrum 2
1.1.2 Gamma radiation and Gamma-ray sources 5
Chapter 2 7
Interactions of gamma with matter 7
2.1 Photoelectric Absorption 8
2.2 Compton Scattering 11
2.3 Pair production 14
Chapter 3 17
Detection Mechanisms of Gamma rays 17
3.1 Scintillation detector 17
3.2 Semiconductor gamma-ray detectors 24
3.2.1 High-purity Ge detectors 25
3.2.2 CdZnTe detectors 27
3.4 Detector resolution 32
Chapter 4 35
Gamma ray Spectrometry 35
4.1 Analysis of natural gamma-ray spectra 35
4.2 Calculation of the Peak Areas of Phootpeaks 38
4.3 Calculation of elemental concentrations (Absolute method) 40
4.4 Calculation of concentration by other methods 42
Chapter 5 43
Application of Gamma ray spectroscopy 43
5.1 Medical Application 43

5.1.1 Scintigraphy (nuclear medicine) 46
5.1.2 Single photon emission CT and single photon emission CT–CT 46
5.1.3 Positron emission tomography (PET) and positron emission tomography–CT 48
5.2 Applications of Neutron Activation Spectroscopy 50
Conclusion 54
Bibliography 55

LIST OF FIGURE

1.1 Distribution (or spectrum) of the intensity of gamma radiation versus the energy of each photon 2
1.2 Schematic representation of the electromagnetic spectrum 3
2.1 A graph depicting the various regions where the different gamma-ray interactions are dominant 8
2.2 Mechanism of photoelectric effect- the incident photon interacts with an orbital electron 10
2.3 Compton scattering diagram showing the relationship of the incident photon and electron initially at rest to the scattered photon and electron given kinetic energy 12
2.4 Mechanism of pair production- the process take place at the Coulomb field of nucleus. 15
3.1 Schematic of a NaI detector and source showing various gamma ray interactions 21
3.2 Pulse Height Analysis 23
3.3 Pulse height spectrum for a monochromatic gamma ray source. 24
3.4a volume of high-purity Ge detectors. 27
3.4b Electronic block diagram of high resolution γ-ray spectrometry system. 27
3.5 A coplanar-grid CdZnTe detectortor. 29
3.6 The coplanar-grid technique for a 1 cm^3 CdZnTe detector. 29
3.7 shows a photograph of a prototype portable detection system. 30
3.8 A comparison of ^{137}Cs spectra obtained from a 24 cm^3 Ge detector and a 1 cm^3 CdZnTe coplanar-grid detector. 30
3.9 Full-energy peak efficiency curve for a germanium detector. 32
3.10 Calculation of FWHM energy resolution of a NaI(TI) detector for 137Cs 662kev γ rays. 33
3.11 The resolution of a scintillator (e.g., NaI or HPGe). 35
4.1 Schematic portion of a natural gamma-ray (NGR) spectrum illustrating the peak definition procedure**.** 38
4.2 Principle of net peak area determination. 40
5.1-a Gamma Camera Overview. 46
5.1-b Gamma-camera Principle. 46
5.2 Gamma ray production. 47
5.3 Single photon emissions CT (SPECT). 49
5.4 Annihilation 50
5.5 Positron emission tomography–CT (PET–CT). 51

Acknowledgements

I would like to express my deep gratitude to my advisor and instructor Dr. Tilahun Tesfaye for his constant assistance, invaluable guidance, useful discussion and encouragement without any reservation during the whole period of my work. It was great pleasure working with him for his keen encouragement, in particular for his available to talk to me and advice or suggestions throughout my work. I also acknowledge financial support for my studies provided by AAU, Natural and computational science faculty, physics department.

I have been very lucky to have some amazing instructors in AAU physics department.

I have learned many things from them like respecting teaching profession, punctuality, encouraging learners to have creative mind and so on. Therefore, I am sure determination and positive attitude will bring them far.

Finally, I have so far received many comments and feedback from all my class mate students, instructors and of course many friends. I have most grateful to them not only for their complements but also for their valuable criticism.

ABBREVIATIONS

ADC	Amplitude-to-digital converter
ADCs	Analog to Digital Convertor
CdZnTe	Cadmium zinc telluride
CSI	Cesium Iodide
CT	computed tomography
DMSA	Dimercaptosuccinic acid
ECG	electrocardiography
FDG	fluorodeoxyglucose
FWHM	full width half max
(Ge (Li))	Lithium-drifted Ge
HDP	hydroxymethylene diphosphonate
HDP	hydroxymethylene diphosphonate
HPGe	high-purity Ge
HV	high voltage
IAEA	International Atomic Energy Agency
LBNL	Lawrence Berkeley National Laboratory
LiI	Lithium Iodide
LVEF	left ventricle ejection fraction
MCA	multi-channel analyzer
MDP	methylene diphosphonate
MRI	magnetic resonance imaging
NaI	Sodium Iodide
[NaI (Tl)]	Thallium-doped Sodium Iodide
NASA	National Aeronautics and Space Administration
PET	positron emission tomography
PHA	Pulse Height Analyzer
PMT	photomultiplier tube
PYP	pyrophosphate
RBC	Red blood cells
ROI	Region of interest
(Si (Li))	Lithium-drifted Si
SPECT	Single photon emission computed tomography
STP	Standard temperature and pressure
UNESCO	United Nations Educational, Scientific and Cultural Organization
ZnS	Zinc Sulfide

ABSTRACT

Gamma-ray spectroscopy is the chief experimental technique of atomic physics and studies the high energy photons which are characteristic of the specific initial- and final-state nuclear energy levels, from radioactive decays. In this review the origin of gamma rays, interaction of gamma with matter, detection mechanism of gamma rays, gamma spectrometry, and applications of gamma-ray spectroscopy are reviewed. In this work, the current status of research in the development of CdZnTe, [NaI (Tl)], and high-purity Ge detectors, by a comprehensive survey on the material properties, the device characteristics, the different techniques for improving the overall detector performance and some major applications are revised.

KEYWORDS: Gamma ray spectroscopy, Origin, Interaction, Detection Application.

Chapter 1

Introduction

Gamma spectroscopy is the science (or art) of identification and/or quantification of radionuclides by analysis of the gamma-ray energy spectrum produced in a gamma-ray spectrometer. It is a widely used technique, well-illustrated by the following list of examples:

* Environmental Radioactivity Monitoring
* Health Physics personnel monitoring
* Reactor Corrosion Monitoring
* Nuclear Materials Safeguards and Homeland Security
* Material Testing
* Geology and Mineralogy
* Nuclear Medicine and Radiopharmaceuticals
* Industrial Process Monitoring

Spectroscopy is the measurement and interpretation of electromagnetic radiation absorbed, scattered, or emitted by atoms, or other chemical species. This absorption or emission is associated with changes in the energy states of the interacting chemical species and, since each species has characteristic energy states, here the electromagnetic radiation is gamma-rays. The study and analysis of gamma-ray spectra for scientific and technical use are by the help of gamma-ray spectrometers. The energy range of the vast majority of gamma-rays from nuclear decay is roughly 10 to 3000 keV. Some gamma-rays of potential interest of up to 12,000 keV occur as a result of nuclear reactions. High energy photons can penetrate rather substantial thicknesses of most materials, it makes them easier to study since they can easily escape the radioactive source and get into detectors. There will be characteristic energy gammas for each nucleus thus useful for identifying radionuclides. By measuring the energy of the emitted gammas, determine which nuclei are in the sample [1]. Gamma-ray spectroscopy minimizes or eliminates the separation required than other methods. These procedures are usually accurate and of widespread applicability in scientific and technical field. Gamma spectroscopy refers to the process of using the energies of gamma rays to identify radionuclides.

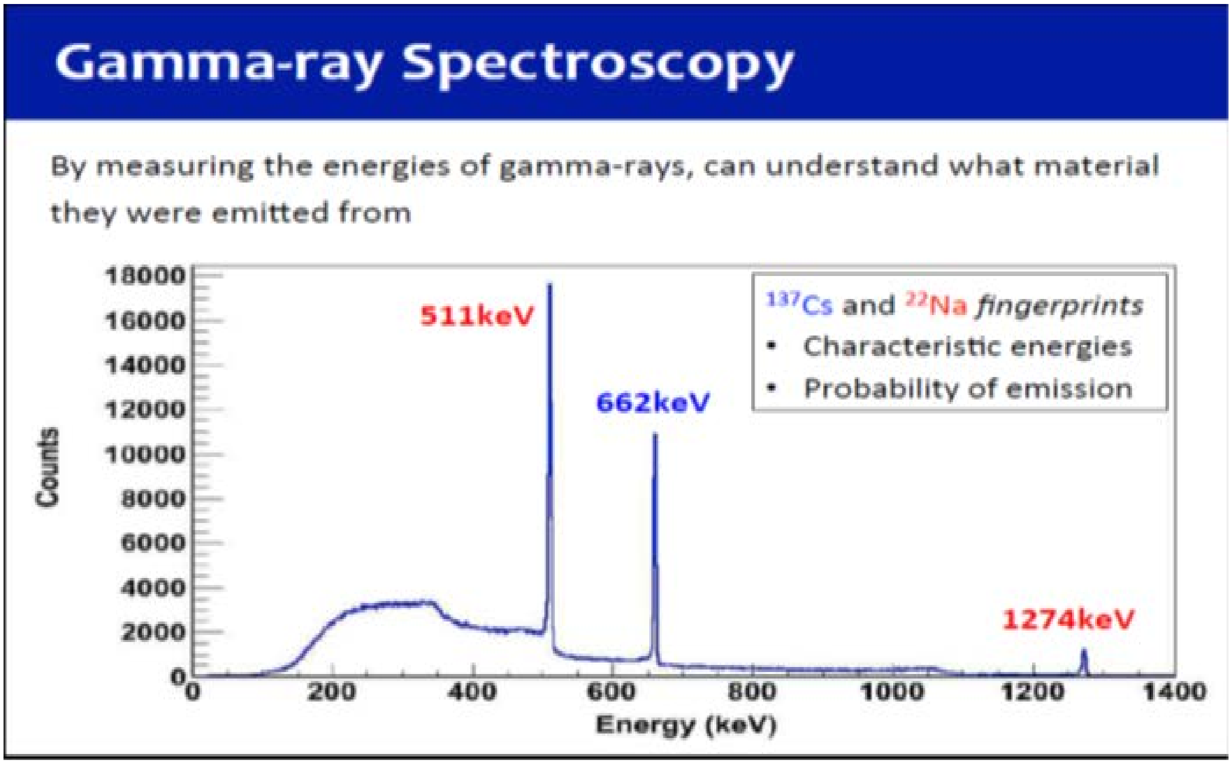

Gamma-ray Spectroscopy

By measuring the energies of gamma-rays, can understand what material they were emitted from

Figure 1.1: Distribution (or spectrum) of the intensity of gamma radiation versus the energy of each photon [2].

Radionuclides must emit gamma rays to be analyzed directly by gamma spectroscopy. Gamma-rays are like fingerprints, they have specific energies that can be used to identify the radioactive material. Gamma spectroscopy is less expensive, fast, non-destructive and multinuclide analysis (all the gamma emitters can be analyzed at once) [3].

1.1 Origin of gamma rays

1.1.1 Gamma-rays and electromagnetic spectrum

Gamma-rays are electromagnetic radiation of the highest energy, with the shortest wavelength and highest frequency. These characteristics make them extremely hazardous to life. They occur on Earth when cosmic rays hit our atmosphere and interact with atoms and molecules in the atmosphere. They are also a by-product of the decay of radioactive elements as in natural radioactive decays, nuclear reactors and nuclear explosions [4].

Gamma-rays are high-energy electromagnetic radiation emitted in the deexcitation of the atomic nucleus. Electromagnetic radiation includes such diverse phenomena as radio, television, microwaves, infrared, light, ultraviolet, X- ray, and gamma-ray. These radiations all propagate through vacuum with the speed of light [4]. They can be described as wave phenomena involving electric and magnetic field oscillations analogous to mechanical oscillations such as water waves or sound. They differ from each other only in the frequency of oscillation. Although given different names, electromagnetic radiation actually forms a continuous spectrum, from low frequency radio waves at a few cycles per second to gamma-rays at 10^{20} Hz and above (see Figure 1.2). The parameters used to describe an electromagnetic wave frequency, wavelength, and energy are related and maybe used interchangeably. It is common practice to use frequency or wavelength for radio waves, color or wavelength for light waves (including infrared and ultraviolet), and energy for X- rays and gamma-rays.

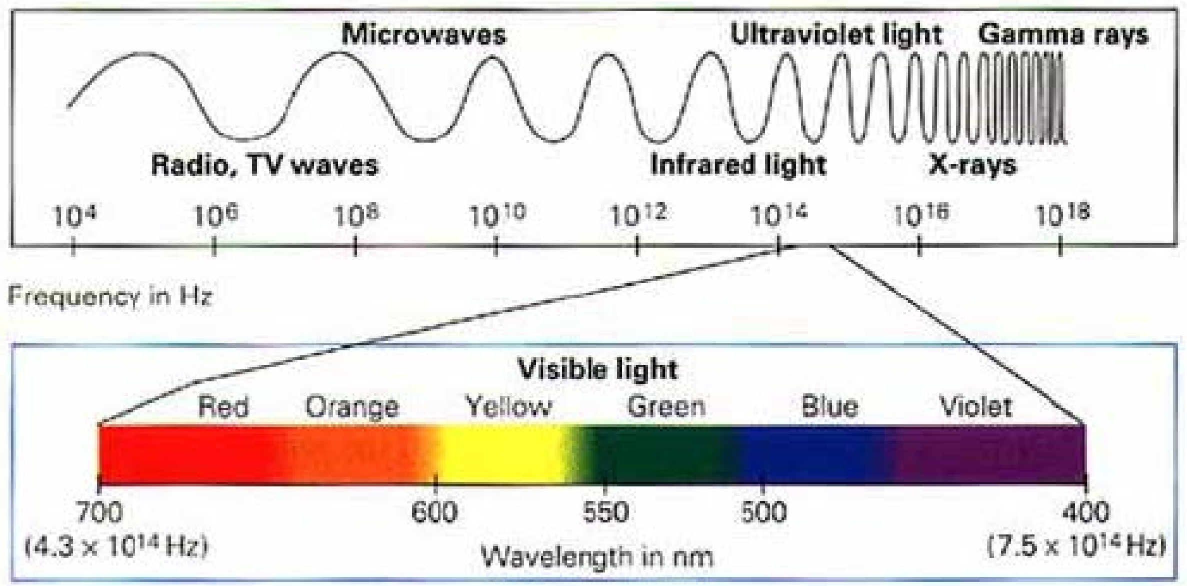

Figure 1.2: Schematic representation of the electromagnetic spectrum [4].

Visible light is emitted during changes in the chemical state of elements and compounds. These changes usually involve the outermost and least tightly bound atomic electrons. The colors of the emitted light are characteristic of the radiating elements and compounds and typically have energies of about 1 eV. X-rays and gamma-rays are very high energy light with overlapping energy ranges of 10 keV and above. X-rays are emitted during changes in the state of inner or more tightly bound electrons, whereas gamma-rays are emitted during changes in the state of nuclei. The energies of the emitted radiations are characteristic of the radiating elements and nuclides.

Knowledge of these high-energy electromagnetic radiations began in Germany in 1895 with the discovery of X-rays by Wilhelm Roentgen [5]. After observing that a zinc sulfide screen glowed when it was placed near a cathode-ray discharge tube, Roentgen found that the radiation that caused the glow was dependent on the electrode materials and the tube voltage, that it was not bent by electric or, magnetic fields, and that it could readily penetrate dense, matter. Natural radioactivity was discovered the following year in France by Henri Becquerel, who observed that Uranium salts gave off a natural radiation that could expose or blacken a photographic plate. While studying these phenomena, Marie and Pierre Curie isolated and identified the radioactive elements Polonium and Radium. They determined that the phenomena were characteristic of the element not its chemical form [6][7].

These “radioactive rays” were intensely studied in many laboratories. In 1899 in England, Ernest Rutherford discovered that 95% of the radiation was effectively stopped by 0.02 mm of aluminum and 50% of the remaining radiation was stopped by 5 mm of aluminum or 1.5 mm of copper. Rutherford named the first component “alpha”, and the second, more penetrating radiation, “beta.” Both these radiations were deflected by electric and magnetic fields, though in opposite directions; this fact indicated that the radiations carried electrical charge.

Gamma-ray is discovered by French chemist and physicist, Paul Ulrich Villard in 1900 while studying the radiation emanating from Radium, Polonium and Uranium. He finds that gamma-ray cannot be deflected by magnetic fields. Paul Villard and Henri Becquerel noted that a photographic plate was affected by radioactive materials even when the plate was shielded by 20 cm of iron or 2 to 3 cm of lead [8]. In 1903 New Zealand-born chemist and physicist Ernest Rutherford named this component “gamma” aid stated that “gamma-rays are probably like Roentgen rays.” Thus the three major radiations were identified and named for the first three letters of the Greek alphabet: α, β and γ. As indicated by the brief description of their discovery, gamma rays often accompany the spontaneous alpha or beta decay of unstable nuclei. X rays are identical to gamma-rays except that they are emitted during rearrangement of the atomic electron structure rather than changes in nuclear structure [9].

The electron volt (eV) is a unit of energy equal to the kinetic energy gained by an electron accelerated through a potential difference, of 1 V; 1 eV equals 1.602×10^{-19} J. This small unit and the multiple units keV (10^3 eV) and MeV (10^6 eV) are useful for describing atomic and molecular phenomena [10]. Gamma-rays from spontaneous nuclear decay are emitted with a rate and energy (color) spectrum that is unique to the nuclear species that is decaying. This uniqueness provides the basis for most gamma-ray assay techniques: by counting the number of gamma-rays emitted with a specific energy, it is possible to determine the number of nuclei that emit that characteristic radiation.

1.1.2 Gamma radiation and Gamma-ray sources

A gamma-ray is a packet (or photon) of electromagnetic radiation emitted from the nucleus during radioactive decay and occasionally accompanying the emission of an alpha or beta particle. Gamma-rays are identical in nature to other electromagnetic radiations such as light or microwaves but are of much higher energy. Examples of gamma emitters are Cobalt-60, Zinc-65, Cesium-137, and Radium-226. Because gamma radiation loses energy slowly, gamma-rays are able to travel significant distances. Depending upon their initial energy, gamma-rays can travel tens or hundreds of meters in air. Gamma radiation is typically shielded using very dense materials (the denser the material, the more chance that a gamma ray will interact with atoms in the material) such as lead or other dense metals. Gamma radiation particularly can present a hazard from exposures external to the body [11].

Gamma-rays are produced primarily by four different nuclear reactions: **fusion, fission, alpha decay** and **gamma decay**.

1. ***Nuclear fusion*** is the reaction that powers the sun and stars. It occurs in a multistep process in which four protons, or hydrogen nuclei, are forced under extreme temperature and pressure to fuse into a helium nucleus, which comprises two protons and two neutrons. The resulting helium nucleus is about 0.7 percent less massive than the four protons that went into the reaction. That mass difference is converted into energy according to Einstein’s famous equation $E = mc^2$, with about two-thirds of that energy emitted as gamma-rays. (The rest is in the form of neutrinos, which are extremely weakly interacting particles with nearly zero mass [12].)

2. ***Nuclear fission*** is another familiar source of gamma-rays. Lawrence Berkeley National Laboratory defines nuclear fission as “the splitting of a heavy nucleus into two roughly equal parts (which are nuclei of lighter elements), accompanied by the release of a relatively large amount of energy in the form of kinetic energy of the two parts and in the form of emission of neutrons and gamma-rays.” In this process, heavy nuclei, such as Uranium and Plutonium, are broken into smaller elements, such as Xenon and Strontium, in collisions with other particles.

The resulting particles from these collisions can then impact other heavy nuclei, setting up a nuclear chain reaction. Energy is released because the combined mass of the resulting particles is less than the mass of the original heavy nucleus. The mass difference is converted to energy in the form of kinetic energy of the smaller nuclei, neutrinos and gamma-rays.

3. ***Alpha decay*** occurs when a heavy nucleus gives off a Helium-4 nucleus, reducing its atomic number by 2 and its atomic weight by 4. This process can leave the nucleus with excess energy, which is emitted in the form of a gamma-ray.

4. ***Gamma decay*** occurs when there is too much energy in the nucleus of an atom, causing it to emit a gamma-ray without changing its charge or mass composition. When gamma rays are produced from radioactive materials, it is through a process called **gamma decay.** Like the electron cloud of an atom, a nucleus can exist in a number of quantized energy states. The lowest of these is called the ***ground state***, and the ones lying above it are ***excited states***. And like an excited atomic electron cloud, an excited nucleus can often get rid of excess energy directly and easily by emitting a high-energy photon, ***a gamma ray, γ***.

Alpha or beta emission brings about a change in the numbers of protons and neutrons present, hence a new overall charge in the resulting daughter nucleus. The new nucleus that an alpha or beta decay leaves behind, moreover, is almost always in an energetically excited state. This daughter nucleus can usually drop immediately into a state of lower energy, however, through the emission of ***a gamma-ray photon***. Indeed, alpha and beta events are usually followed almost instantaneously (typically in less than a millionth of a second) by the emission of ***a gamma-ray*** [13].

Chapter 2

Interactions of gamma with matter

Knowledge of gamma-ray interactions is important in order to understand gamma-ray detection and attenuation. A gamma-ray must interact with a detector in order to be “seen.” It is, however, essential that the interaction be understood in order to apply the knowledge to γ-spectrometry. Gamma photons produce ionization indirectly as a result of collisions. The Basic mechanism for the detection of ionizing radiation is the transfer of energy to material.

The gamma-rays of interest to applications fall in the range 10 to 2000 keV and interact with detectors and absorbers by three major processes:

- ***Photoelectric absorption***
- ***Compton scattering, and***
- ***Pair-production.***

Which of these processes contributes the most is mainly dependent on the atomic number (Z) of the material and the energy (E) of the photon. In the photoelectric absorption process, the gamma ray loses all of its energy in one interaction. The probability for this process depends very strongly on gamma-ray energy E_γ and atomic number Z. In Compton scattering, the gamma ray loses only part of its energy in one interaction [14]. The probability for this process is weakly dependent on E and Z. The gamma ray can lose all of its energy in one pair-production interaction. However, this process is relatively unimportant for fissile material assay since it has a threshold above 1 MeV. $E < 1.022$ MeV: Compton and Photoelectric interactions are possible. But $E > 1.022$ MeV with Pair production**.**

These different interactions change their probability of occurring depending on the energy of the gamma-ray and the atomic number of the material. Figure 2.1, a graph depicting the various regions where the different gamma-ray interactions are dominant. As can be seen from Figure 2.1, the photoelectric effect is dominant for low energy photons and high Z materials. Pair production is dominant for high energy photons and high Z materials. The Compton scattering interaction is dominant for moderate energies**.**

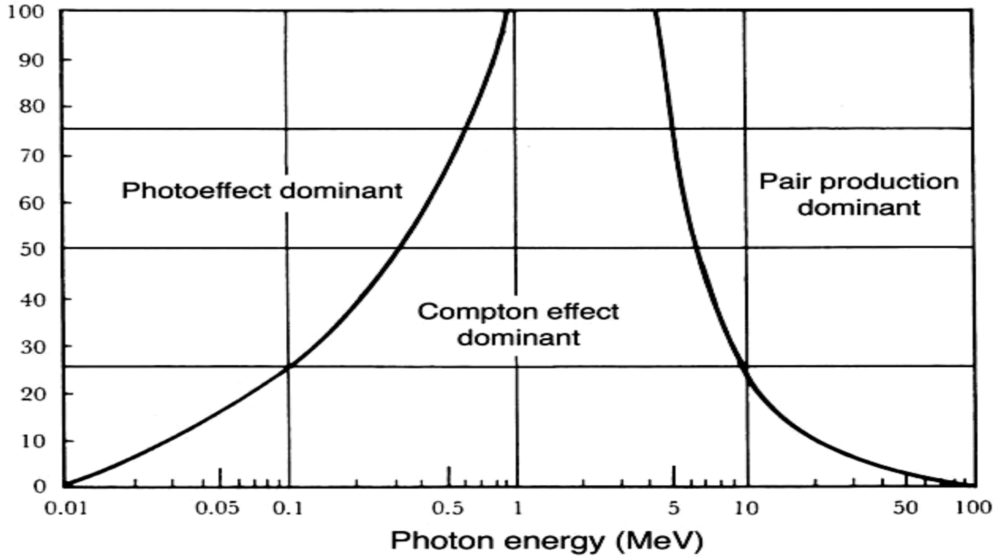

Figure 2.1: A graph depicting the various regions where the different gamma-ray interactions are dominant [15].

2.1 Photoelectric Absorption

Atomic electrons are removed from their nuclei, thus reducing the energy of the γ-ray photon by the electron's binding energy. This is the dominant process at energies below 100 keV. A gamma-ray may interact with a bound atomic, electron in such a way that it loses all of its energy and ceases to exist as a gamma ray (see Figure 2.2). Some of the gamma-ray energy is used to overcome the electron binding energy, and most of the remainder is transferred to the freed electron as kinetic energy. A very small amount of recoil energy remains with the atom to conserve momentum. This is called photoelectric absorption because it is the gamma-ray analog of the process discovered by Hertz in 1887 whereby photons of visible light liberate electrons from a metal surface. Photoelectric absorption is important for gamma-ray detection because the gamma ray gives up all its energy, and the resulting pulse falls in the full-energy peak. The probability of photoelectric absorption depends on the gamma-ray energy, the electron binding energy, and the atomic number of the atom. The probability is greater the more tightly bound the electron therefore; K-shell electrons are most affected provided the gamma-ray energy exceeds the K-shell electron binding energy [16]. The probability is given approximately by Equation 2.1, which shows that the interaction is more important for heavy atoms like Lead and Uranium and low-energy gamma rays:

$$\tau \,\alpha\, Z^4/(hv)^3 \,, \qquad (2.1)$$

where τ = photoelectric, mass attenuation coefficient [17]. The proportionality is only approximate because the exponent of Z varies in the range 4.0 to 4.8. Photoelectric absorption is the predominant interaction for low-energy gamma rays and high Z materials.

The energy of the photoelectron E_e released by the interaction is the difference between the gamma-ray energy E_γ and the electron binding energy E_b:

$$E_e = E_\gamma - E_b, \tag{2.2}$$

where, E_b denotes the energy required to remove a bound electron from that atom [18].
In this effect it is the binding energy for the K- and L-shell electrons to that atom.
The high energy electron is in all respects the same as a β-particle, and can cause secondary ionization in the medium. It is assumed that this electron will lose all its energy in the material. It is important to note that the photon "disappears" in this process.

In photoelectric absorption the incident photon disappears and a photoelectron is ejected from one of the electron shells of the absorber (Figure 2.2). The kinetic energy, E_e of the photoelectron is given by the equation $E_e = hv - E_b$, where hv is the photon’s energy and E_b is the binding energy of the liberated electron in its original shell. The atom is left in an excited state with an excess energy of E_b and recovers its equilibrium in two ways; the atom may de-excite by redistribution of the excitation energy between the remaining electrons in the atom resulting in release of further electrons (Auger cascade) which transfers a further fraction of total energy to detector or vacancy left by ejection of the photoelectron may be filled by higher energy electron falling into it with emission of characteristic X-ray fluorescence.

The photoelectric effect involves mainly those electrons that are closely bound to the nucleus (i.e. the inner orbitals) in the K- and L-shells. The probability for the effect becomes less for the electrons that are more loosely bound in outer orbitals. If the energy of the incident photon is less than the ionization potential or binding energy of an electron in a particular inner shell, that electron cannot be involved in the photoelectric effect

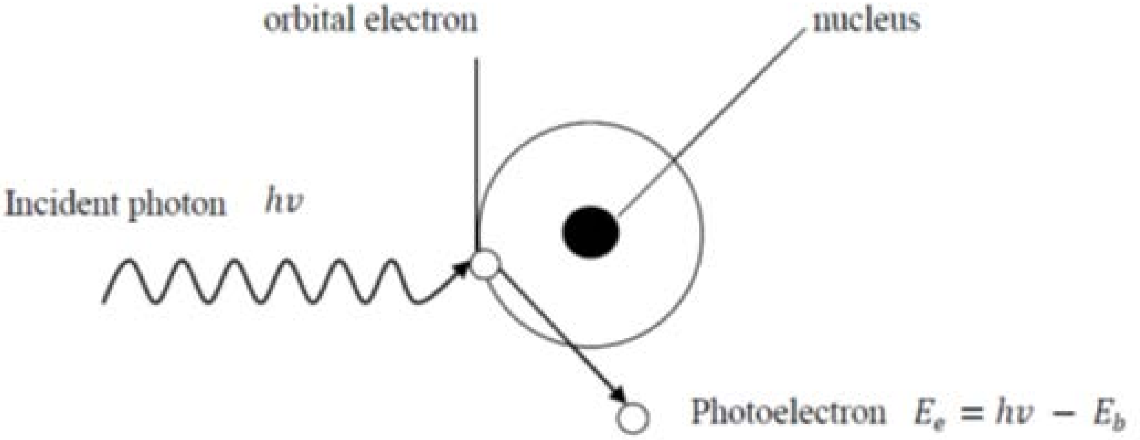

Figure 2.2: Mechanism of photoelectric effect- the incident photon interacts with an orbital electron [18].

The probability for the photoelectric effect is also determined by a number of other aspects such as the higher the energy of the incident photon (above the $h\upsilon > E_{b\ \text{limit}}$), the smaller the chance for the effect to occur, and the higher the atomic number of the absorbing material, the bigger the chance for the effect. This can be summarized by the following equation above the low-energy absorption edges:

$$\text{Probability of the effect} = K\,(Z^5/E^{3.5}), \qquad (2.3)$$

where, Z is the atomic number of the absorbing material; and E is the energy of the photon [18].

In photoelectric effect we can see that all of the energy of the incoming photon is totally transferred to the atom and following interaction, the photon ceases to exist. The incoming photon interacts with an orbital electron in an inner shell – usually K and the orbital electron is dislodged. The ejected electron is now a photoelectron and this photoelectron can interact with other atoms until all its energy is spent. A vacancy now exists in the inner shell, then to fill this gap, an electron from an outer shell drops down to fill the gap and once the gap is filled, the electron releases its energy in the form of a characteristic photon. This process continues, with each electron emitting characteristic photons, until the atom is stable. Therefore; the byproducts of the photoelectric effect are photoelectrons and characteristic photons. The Probability of occurrence depends on the energy of the incident photon, the atomic number of the irradiated object, and it increases as the photon energy decreases, and the atomic number of the irradiated object increases.

2.2 Compton Scattering

Electrons are hit by the γ-ray photons, and gain a fraction of the photon's kinetic energy in this collision. This is the dominant interaction process in the 0.1 MeV to a few MeV regimes. Compton scattering is the process whereby a gamma ray interacts with a free or weakly bound electron ($E_\gamma >> E_b$) and transfers part of its energy to the electron (see Figure 2.3). Conservation of energy and momentum allows only a partial energy transfer when the electron is not bound tightly enough for the atom to absorb recoil energy. This interaction involves the outer, least tightly bound electrons in the scattering atom. The electron becomes a free electron with kinetic energy equal to the difference of the energy lost by the gamma ‘ray and the electron binding energy. Because the electron binding energy is very small compared to the gamma-ray energy, the kinetic energy of the electron is very nearly equal to the energy lost by the gamma ray:

$$E_e = E_\gamma - E', \qquad (2.4)$$

where, E_e is the energy of scattered electron, E_γ is the energy of incident gamma ray, and E' is the energy of scattered gamma ray.

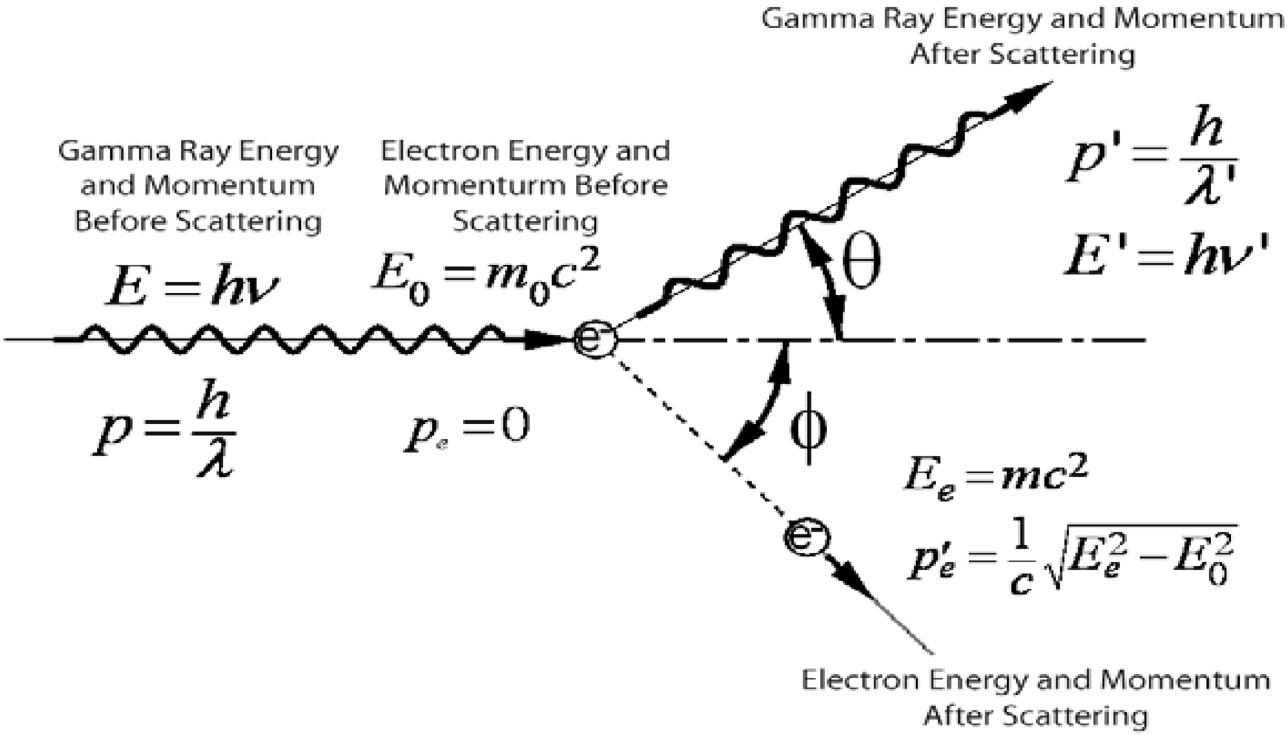

Figure 2.3: Compton scattering diagram showing the relationship of the incident photon and electron initially at rest to the scattered photon and electron given kinetic energy [17].

Two particles leave the interaction site: the freed electron and the scattered gamma ray. The directions of the electron and the scattered gamma ray depend on the amount of energy transferred to the electron during the interaction. Equation 2.4 gives the energy of the scattered gamma-ray.

$$E' = m_oc^2/\,(1 - \cos\theta + m_oc^2/E), \qquad (2.5)$$

where m_oc^2 = 511 keV is the rest energy of electron, θ is the angle between incident and scattered gamma-rays (see Figure 2.3).

This energy is minimum for a head-on collision where the gamma ray is scattered 180° and the electron moves forward in the direction of the incident gamma ray. For this case the energy of the scattered gamma ray is given by Equation 2.5 and the energy of the scattered electron is given by Equation 2.6:

$$E'\,(\text{min}) = m_oc^2/(2 + m_oc^2/E)$$

$$\approx m_oc^2/2 = 256\ \text{keV};\ \text{if } E >> m_oc^2/2 \qquad (2.6)$$

$$E_e(\max) = E/[1 + m_oc^2/(2E)]$$

$$\approx E - m_oc^2/2 = E - 256 \text{ keV; if } E >> m_oc^2/2 \qquad (2.7)$$

The absorption cross-section for Compton scattering σ is related to the atomic number Z of material and energy $h\nu$ of the gamma ray by equation 2.8

$$\sigma \;\alpha\; Z/\,h\nu \qquad (2.8)$$

The photon is reflected (or scattered) through an angle (θ) with respect to the line of incidence (Figure 2.3), and moves along with decreased energy. If the photon with energy E is treated as a wave with wavelength, Compton scattering can be described by:

$$(\lambda - \lambda_0) = h/mc\ (1 - \cos\theta)\ , \text{ where } E_\gamma = h\nu = hc/\lambda \qquad (2.9)$$

If the scattering angle θ is known, it is then possible to calculate from standard mechanics: (i) the angle at which the electron is moving, and (ii) the ratio in which the available energy (from the incident photon) is divided between the electron and the scattered photon [18].

The maximum energy that a photon can transfer to an electron is when $\theta = 180^0$, i.e., when the photon is scattered directly backwards (and the electron moves in the direction of the incident photon). This is still less than the total energy that can be transferred by the same photon in a photoelectric interaction. The scattering angle can have values in the range between 0 and 180^0. And the smaller the angle, the smaller the amount of energy that is transferred to the electron. A photon just "grazing" an electron (θ=0) transfers no energy [16].

The probability for Compton interaction increases with the atomic number of the absorber, and decreases with the energy of the incident photon. This can be summarized by:

Probability of the effect = K (Z/E)

An interesting situation develops for the geometric arrangements normally used for counting samples: the sample is placed close to the detector inside a heavy shield (normally Lead). The detector therefore "sees": (i) photons directly from the sample, and (ii) a smaller number that were all reflected by approximately 180^0 from the absorber**.** This backscattering produces photons with more or less the same energy, regardless of the energy of the photons incident on the Lead shield. The backscattered photons appear as a broad peak in the low-energy region of the pulse height spectrum [17].

In Compton scattering we can observe that, an incoming photon is partially absorbed in an outer shell electron and the electron absorbs enough energy to break the binding energy, and is ejected. The ejected electron is now a Compton scattered electron and it possesses kinetic energy and is capable of ionizing atoms and finally recombines with an atom that has an electron deficiency. The incoming photon continues on its way, but in a different direction with lower energy as scattered gamma-ray photon and it can interact with other atoms, either by photoelectric or Compton scattering.

2.3 Pair production

Pair production predominates for high-energy gamma rays (above 5 - 10 MeV). In the presence of an electric field (usually of the atomic nucleus), the γ-ray energy may be converted into particle antiparticle pair, electron and positron. From momentum conservation, these two particles move in opposite directions so that the momentum component perpendicular to the γ-ray cancels; transformation into the laboratory system makes them appear to fork out of the γ-ray's incidence direction with a narrow opening angle, which decreases with energy. This interaction process cannot occur below a threshold of 1.022 MeV, and the cross section increases with energy so that it dominates over Compton scattering above several MeV. The same process can occur in dense photon fields through collisions of energetic photon.

Pair production results from interaction of the gamma-ray with the atom as a whole. The process takes place within the Coulomb field of the nucleus, resulting in the conversion of a gamma-ray into an electron-positron pair (Figure 2.4). The energy of the gamma-ray must be at least twice the rest mass of an electron which is 1022 keV. The electron and positron created share the excess gamma-ray energy (i.e. the energy in excess of the combined electron–positron rest mass) equally, losing it to the medium as they are slowed down.

The cross-section ƙ dependence for the pair production on Z as given by:

$$\text{Ƙ} \ \alpha \ Z^2 \tag{2.9}$$

A high-energy gamma photon sometimes changes into two electrons, one positive and the other negative. The positive electron is called the positron. This interaction is known as pair production, for obvious reasons [18]. This effect can be explained in terms of the relativity theory (Albert Einstein) which postulates that "matter" and "energy" are different forms of the same entity. A particle of mass m can be converted into an amount of energy E, and vice versa, according to the equation $E = mc^2$, where c is the speed of light.

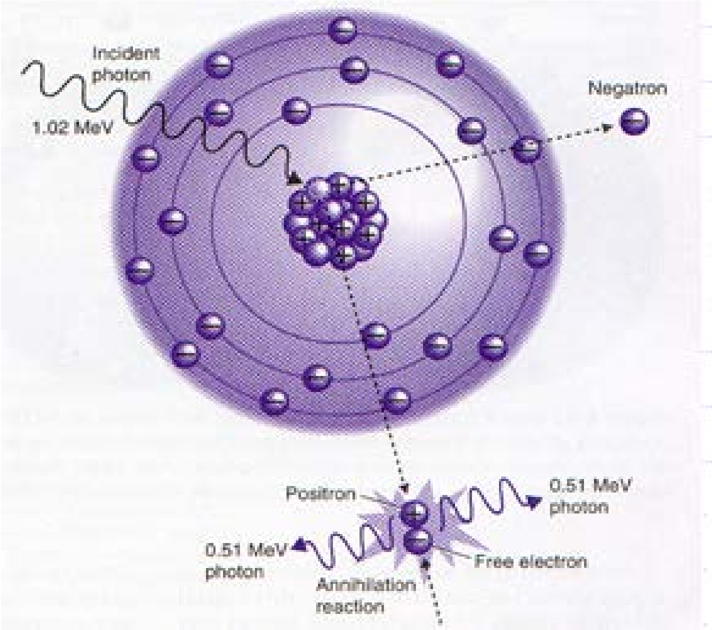

Figure 2.4: Mechanism of pair production the process take place at the Coulomb field of nucleus [19].

Pair production is one consequence of this theory: a photon with energy E is converted into two different particles with the same mass, but with opposing electrical charges. The excess energy (i.e., more than the minimum required to produce the particles) is shared by the two particles in the form of kinetic energy:

$$E_{e-} + E_{e+} = h\upsilon - 2m_0c^2 \quad \text{or} \quad E_\gamma = (m_+ + m_-)\,c^2 + (\tfrac{1}{2}\,mv^2)_+ + (\tfrac{1}{2}\,mv^2)_-$$

The two particles involved are both electrons. One, the electron, is negatively charged, the other, is the positive electron, or positron. It has the same mass and nuclear properties as the negative electron, but with the opposite electrical charge. The term negatron is sometimes used to distinguish the negative from the positive electron [19].

The amount of energy equivalent to the mass of the electron or positron (= 9.11×10^{-28} g) can be calculated from the Einstein equation. It amounts to 511 keV for one particle; or 1022 keV for a positron-negatron pair. The equation above can therefore be written as

$$E_\gamma = 1022 + (\tfrac{1}{2}\,mv^2)_+ + (\tfrac{1}{2}\,mv^2)_-$$

All energy values are in keV [10].

The positron at rest is not a stable particle. Once it is has been produced by pair production, the positron will lose energy by interaction with electrons in the absorbing material in the same manner that a negatron does. But when it has lost all its kinetic energy, it cannot exist in the presence of other electrons, and a nuclear reaction occurs. In this reaction a positron and negatron pair destroys (annihilates) each other with the production of two photons with energy of 511 keV each. (*This annihilation can occur between the positron and any electron; not necessarily with the one formed during the pair production* [20].)

There are two photons involved in order to conserve momentum during the reaction. It can be represented by

$$\beta^{+} + \beta^{-} \rightarrow \gamma_1 + \gamma_2 \qquad \text{and} \qquad E\gamma_1 = E\gamma_2 = 511 \text{ keV}$$

Pair production is only possible if the energy of the incident photon is sufficient to provide at least the mass of a positron and negatron pair (> 1022 keV). In practice it is only significant for photon energies above 1.5 MeV. The higher the photon energy, the more likely pair production is to occur. The likelihood varies roughly as $(E - 1.02)^2Z^2$.

In Pair Production we can see that the incoming photon must have energy of at least 1.02 MeV interacts with the nucleus of an atom and this process is a conversion of energy into matter and then matter back into energy. In this interaction the incoming photon disappears and the transformation of energy results in the formation of two particles Negatron (possesses negative charge) and Positron (possesses a positive charge). An electron and the positron destroy each other during interaction which is known as the annihilation reaction. This converts matter back into energy and both the positron and electron disappear each other, and then the two gamma photons are released with energy of .51 MeV. The produced gamma photons may interact with matter through pair production or Compton scatter. Pair production is used for positron emission tomography, a nuclear medicine imaging procedure and it is also used in radiation therapy.

Chapter 3

Detection Mechanisms of Gamma rays

The detection of γ-rays is of considerable importance, not just in studies of nuclear physics but in many applications as well. In general two main characteristics are of importance in the design of systems to detect them, namely ***energy resolution and efficiency.*** More recently it has become important to have detectors, which allow us to determine the initial direction of the interacting γ-rays. In application to nuclear physics this allows us to correct the measured energy according to how fast the emitting source is moving. In other applications it is important in terms of pinpointing the source of radiation [21].

In order for a gamma ray to be detected, it must interact with matter that interaction must be recorded. Fortunately, the electromagnetic nature of gamma-ray photons allows them to interact strongly with the charged electrons in the atoms of all matter. The key process by which a gamma ray is detected is ionization, where it gives up part or all of its energy to an electron. The ionized electrons collide with other atoms and liberate many more electrons. The liberated charge is collected, either directly (as with a proportional counter or a solid-state semiconductor detector) or indirectly (as with a scintillation detector), in order to register the presence of the gamma ray and measure its energy [21]. ***The final result is an electrical pulse whose voltage is proportional to the energy deposited in the detecting medium***. Detection of gamma radiation is one of the most important research tools in nuclear physics. Detection of gamma radiation yields information on various properties (excitation energies, angular moments, decay properties etc.) of states in nuclei. In this review we will become familiar with two different detectors used for observing gamma radiation (***scintillation and semiconductor detectors***) and compare the properties of these detectors.

3.1 Scintillation detector

Scintillators are materials that produce ‘small flashes of light’ when struck by ionizing radiation (e.g. particle, gamma, neutron). This process is called ‘Scintillation’. Scintillators may appear as solids, liquids, or gases. Major properties for different scintillating materials are light yield and linearity (energy resolution), how fast the light is produced (timing), and detection efficiency.

The sensitive volume of a scintillation detector is a luminescent material (a solid, liquid, or gas) that is viewed by a device that detects the gamma-ray-induced light emissions [usually a photomultiplier tube (PMT)]. The scintillation material may be organic or inorganic; the latter is more common. Examples of organic scintillators are anthracene, plastics, and liquids. The latter two are less efficient than anthracene (the standard against which other scintillators are compared). Some common inorganic scintillation materials are sodium iodide (NaI), cesium iodide (CSI), zinc sulfide (ZnS), and lithium iodide (LiI). The most common scintillation detectors are solid, and the most popular are the inorganic crystals NaI and CSI. A new scintillation material, bismuth germanate ($Bi_4Ge_3O_{12}$), commonly referred to as BGO, has become popular in applications where its high gamma counting efficiency and/or its lower neutron sensitivity outweigh considerations of energy resolution [22].

When gamma-rays interact in scintillator material, ionized (excited) atoms in the scintillator material “relax” to a lower-energy state and emit photons of light. In a pure inorganic scintillator crystal, the return of the atom to lower-energy states with the emission of a photon is an inefficient process. Furthermore, the emitted photons are usually too high in energy to lie in the range of wavelengths to which the PMT is sensitive. Small amounts of impurities (called activators) are added to all scintillators to enhance the emission of visible photons. Crystal de-excitations channeled through these impurities give rise to photons that can activate the PMT.

One important consequence of luminescence through activator impurities is that the bulk scintillator crystal is transparent to the scintillation light. A common example of scintillator activation encountered in gamma-ray measurements is thallium-doped sodium iodide [NaI(Tl)].

Gamma-ray detection with a NaI (Tl) crystal was discovered by Robert Hofstadter in 1948. Later that year gamma spectroscopy with NaI (Tl) was discovered by Hofstadter and his graduate student, John McIntyre. The basic properties of the detector were researched and reported in the Physical Review over the next few years. Since then the scintillation detector (of which there are many different crystals), in particular the NaI (Tl) detector, have been used in a wonderful array of important physical experiments [19].

The scintillation light is emitted isotropically; so the scintillator is typically surrounded with reflective material (such as MgO) to minimize the loss of light and then is optically coupled to the photocathode of a PMT. (See Figure 3.1.) Scintillation photons incident on the photocathode liberate electrons through the photoelectric effect, and these photoelectrons are then accelerated by a strong electric field in the PMT. As these photoelectrons are accelerated, they collide with electrodes in the tube (known as dynodes) releasing additional electrons. This increased electron flux is then further accelerated to collide with succeeding electrodes, causing a large multiplication (by a factor of 10^4 or more) of the electron flux from its initial value at the photocathode surface. Finally, the amplified charge burst arrives at the output electrode (the anode) of the tube. The magnitude of this charge, surge is proportional to the initial amount of charge liberated at the photocathode of the PMT, the constant proportionality is the gain of the PMT. Furthermore, by virtue of the physics of the photoelectric effect, the initial number of photoelectrons liberated at the photocathode, is proportional to the amount of light incident on the phototube, which, turn, is proportional to the amount of energy deposited in the scintillator by the gamma ray (assuming no light loss from the scintillator volume). Thus, an output signal is produced that is proportional to the energy deposited by the gamma ray in the scintillation medium. As discussed above, however, the spectrum of deposited energies (even for a mono-energetic photon flux) is quite varied, because of the occurrence of the photoelectric effect, Compton effect, and various scattering phenomena in the scintillation medium and statistical fluctuations associated with all of these processes.

The scintillation detector is illustrated in Fig. 3.1. Our detector has a 4×4 inch cylindrical NaI scintillation crystal which is activated with about 1 part in 103 thallium impurities. Through various processes, a gamma ray passing into the crystal may interact with it creating many visible and ultraviolet photons (scintillations).To detect the scintillation photons, the crystal is located next to a photomultiplier tube (PMT) and the scintillator/PMT (detector) is enclosed in a reflective, light-tight housing. To minimize the effects of background gamma radiation, the detector is surrounded by a thick lead shielding tube with the desired gamma rays entering at the scintillator end of the tube.

Some crystals are intrinsic scintillators in which the luminescence is produced by a part of the crystal lattice itself. However, other crystals require the addition of a dopant, typically fluorescent ions such as thallium(Tl) or cerium(Ce) which is responsible for producing the scintillation light (in both cases is the scintillation mechanism the same): The energy is transferred to the luminescent centers which then radiate scintillation photons. For example, in the case of thallium doped sodium iodide (NaI (Tl)), the light output is ~40,000 photons per

MeV deposited energy. This high light output is largely due to the high quantum efficiency of the thallium ion, disadvantage rather slow (250ns) decay time.

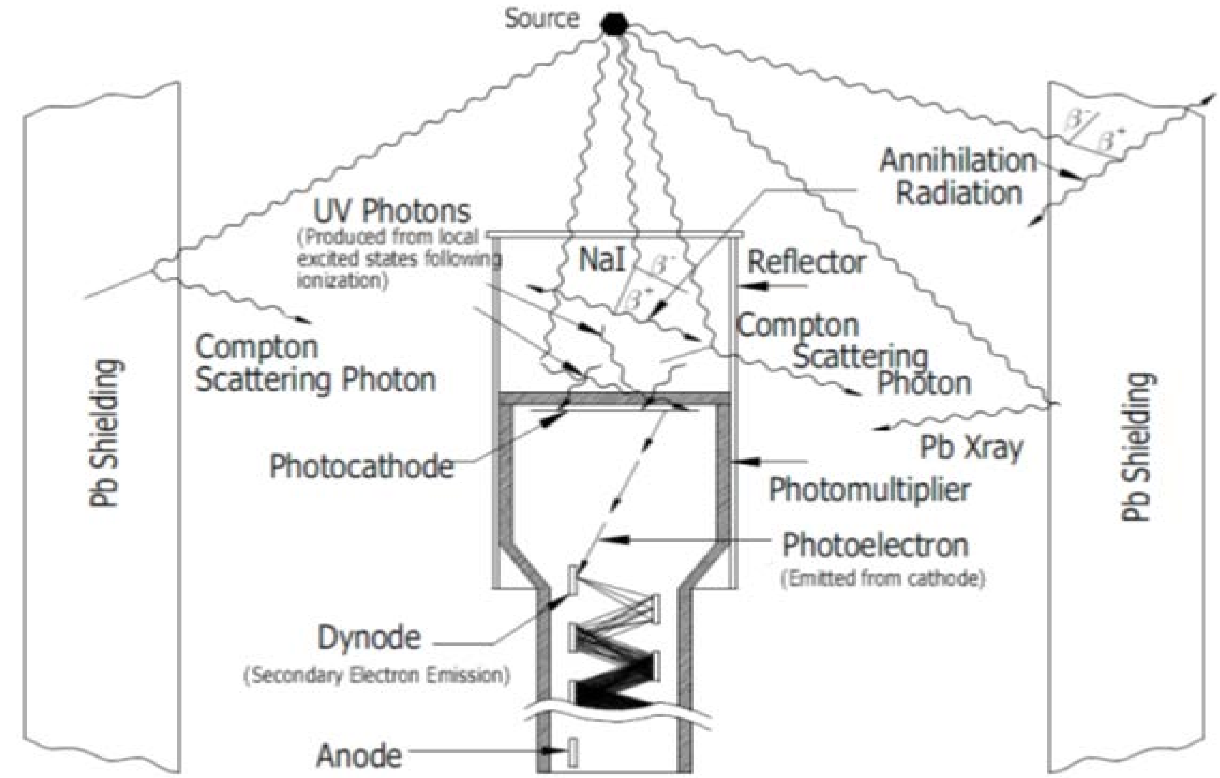

Figure 3.1: Schematic of a NaI (Tl) detector and source showing various gamma ray interactions [21].

The processes which take place within the PMT are the light photon strikes a light sensitive layer, the photocathode, causing it to emit a photoelectron, and the photoelectrons are focused electrostatically onto the first of a series of electron multiplier stages, called ***dynodes***. These emit more electrons than they receive, thus amplifying the signal. The electrons from the first dynode are multiplied at the second dynode, and again at the third, all the way down the chain. The amplified signal is then collected at the ***anode*** and passed out to the measurement circuits.

The design of photomultipliers varies depending upon what they are to measure. For scintillation gamma-ray measurements, they are always of an end-window design with the photocathode deposited on the inside of the face of the tube. The whole structure is enclosed within an evacuated glass envelope and connections made via a multipin plug at the anode end.

The PMT consists of a photocathode followed by a series of dynodes and ending with a collection anode. Scintillation photons striking the photocathode eject electrons via the photoelectric effect. A high voltage (HV) power supply and a resistor chain (not shown) bias the cathode, dynodes, and anode so as to accelerate electrons from the cathode into the first dynode, from one dynode to the next, and from the final dynode to the anode collector. Each incident electron strikes a dynode with enough energy to eject around 5-10 (secondary) electrons from that dynode. For each initial photoelectron, by the end of the chain, there are on the order of 10^6 electrons reaching the anode [19].

The anode is connected to a charge sensitive preamplifier which converts the collected charge to a proportional voltage pulse. The preamplifier pulse is then shaped and amplified by a linear amplifier before processing continues.

Because the amount of light (number of photons) produced in the scintillation crystal is proportional to the amount of gamma-ray energy initially absorbed in the crystal, so also are the number of photoelectrons from the cathode, the final anode charge, and the amplitude of the preamplifier and amplifier voltage pulses. The overall effect is that the final ***pulse height is proportional to the gamma ray energy absorbed in crystal*** [21].

Pulse Height Analyzer

As the name suggests, a pulse height analyzer (PHA) measures the height of each input pulse. Special circuitry, including a sample and hold amplifier and an analog to digital converter, determines the maximum positive height of the pulse a peak voltage as might be read off an oscilloscope trace. From the pulse height, a corresponding channel number is calculated. For example, for a PHA having 1000 channel capability and a pulse height measurement range from 0 to 10 V, a pulse of height 1.00 V would correspond to channel 100, one of 2.00 V would correspond to channel 200, one of 8.34 V would correspond to channel 834, etc [22]. After the correct channel for a given input pulse has been determined, the PHA then increments the count in that channel. Our PHA can analyze pulse heights in the range 0-10 V and will be set up to sort them into 1024 channels.

The different types of ADCs **(Analog to Digital Convertor)** measure the pulse heights in different ways. We will imagine that the ADC measures the size of the pulses with a ruler. The conversion gain is 10. Looking at the following figure, how many pulses will be sorted into each of the ten channels?

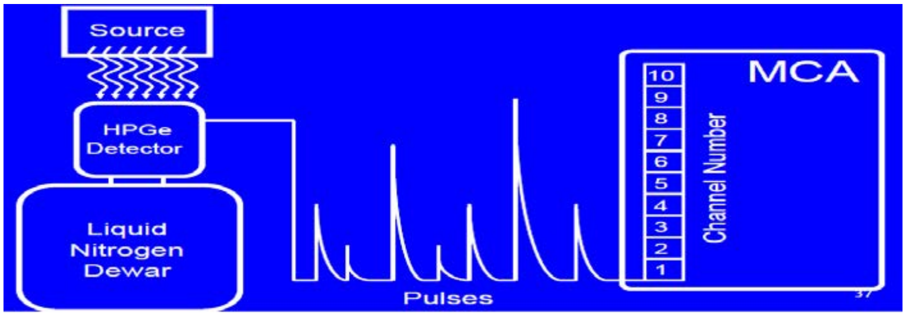

Figure 3.2: Pulse Height Analysis [21].

After many pulses of various sizes have been processed, a plot of the counts in each channel versus the channel number can be displayed to show the distribution of pulse heights. With some caveats to be described shortly, the pulse height distribution from a scintillation detector can be interpreted as a plot of the number of gammas versus the energy of the gammas from the source, i.e., a gamma ray spectrum of the (radioactive) source. Spectra from pure isotopes can be found in references and compared with source spectra to determine the nuclear composition of the source.

Gamma Interactions with the scintillator:

A pulse is produced for each gamma ray interacting in the detector. A pulse is a short-term change in the voltage. The greater the energy deposited in the detector, the larger the pulse. The number of pulses count from the detector can be related to the activity of the radionuclides in the sample (gamma spectrometry). The height of the pulses can be related to the energy of the gamma-rays. This is used to identify the radionuclides in the sample.

To understand the pulse height distribution associated with the gamma-rays from a radioactive source, it is important to realize that only a fraction of the gamma-rays interact with the scintillator; many do not interact at all and simply pass right through. Furthermore, when a gamma does interact, the size of the pulse from the detector depends on whether all or only part of the gamma ray energy is deposited in the scintillator.

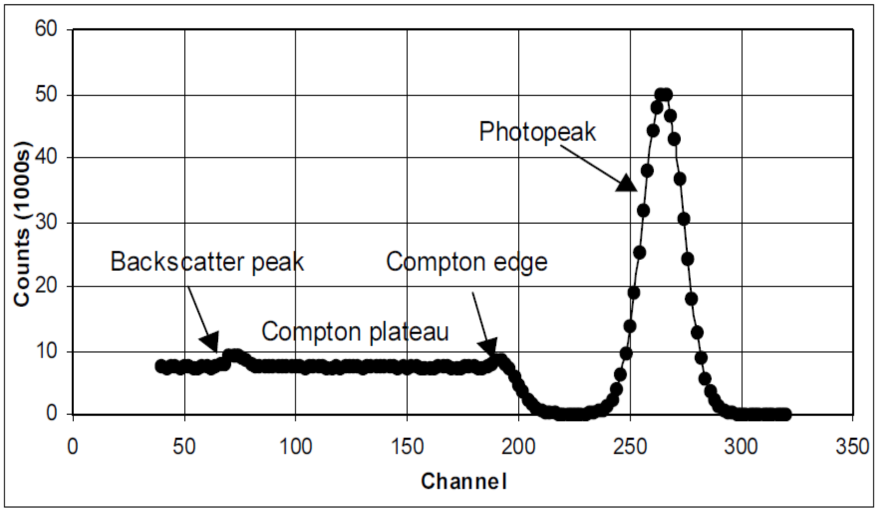

Figure 3.3: Pulse height spectrum for a monochromatic gamma ray source [21].

For a given amount of energy deposited in the scintillator, the output pulse height will be Well-defined but every pulse will not be exactly the same size. Because of statistical variations in light production, photon collection, photoelectron production, and electron multiplication, the pulse heights will show a distribution of values with some pulse heights larger and some smaller than the average. Typical variations of detectors are in the range of 5-10 percent [20].

The pulse height distribution for a source emitting only single energy gamma rays typically appears as in Fig. 3.3. The large peak at the far right is called the photo peak (full-energy peak) and arises when all the gamma ray energy is deposited in the scintillator. Note the 5-10% width of this peak due to statistical fluctuations. The most likely interaction to deposit 100% of the gamma-ray energy is the photoelectric effect. The incident gamma essentially gives up all its energy to eject a bound inner shell electron from one of the crystal atoms. The ejected electron then has significant kinetic energy (the gamma ray energy less the small binding energy of the atomic electron, on the order of 10 keV) and loses this energy by exciting and ionizing more crystal atoms.

Compton scattering is another way gamma-rays can interact in the crystal. The small peak at low voltage (called the backscatter peak) arises when gamma photons first strike the lead shield and then Compton scatter back into the detector. The scattered photons, which are greatly reduced in energy, produce the backscatter peak. The Compton plateau the relatively flat region extending from the Compton edge to lower energies occurs when gamma-rays Compton scatter in the scintillator. The recoiling electron's energy is deposited in the crystal while the scattered photon exits the crystal undetected. The recoil energy varies from a maximum at the Compton edge when the photon backscatters, to zero when the photon is scattered in the forward direction.

The third way gamma-rays interact is through pair production. In the strong electric fields near crystal nuclei, a gamma-ray can create an electron-positron pair as long as the gamma-ray energy exceeds 1.022 MeV (the rest mass energy of an electron and positron). Any gamma energy in excess of this becomes kinetic energy of the electron and positron. This kinetic energy is quickly absorbed in the crystal and when the positron gets to low enough energy, it annihilates with an electron producing two 0.511 MeV gammas. The creation, energy loss, and annihilation effectively occur instantaneously. If both annihilation gammas are absorbed, the total energy absorbed will be the original gamma energy and the event would contribute to the photo peak. However, sometimes either or both of the annihilation gammas will escape from the crystal producing small peaks (called single or double escape peaks) 0.511 MeV or 1.022 MeV below the photo peak [22].

3.2 Semiconductor gamma-ray detectors

The successful development of lithium-drifted Ge detectors in the 1960's marked the beginning of the significant use of semiconductor crystals for direct detection and spectroscopy of gamma rays. In the 1970's, high-purity Ge became available, which enabled the production of complex detectors and multi-detector systems**.** In the following decades, the technology of semiconductor gamma-ray detectors continued to advance, with significant developments not only in Ge detectors but also in Si detectors and room temperature compound-semiconductor detectors. In recent years, the group at Lawrence Berkeley National Laboratory has developed a variety of gamma-ray detectors based on these semiconductor materials. Examples include Ge strip detectors, lithium-drifted Si strip detectors, and coplanar-grid CdZnTe (Cadmium zinc telluride) detectors. These advances provide new capabilities in the measurement of gamma rays, such as the ability to perform imaging and the realization of highly compact spectroscopy systems [23].

Lithium-drifted Ge (Ge(Li)) detectors were developed and successfully used for gamma -ray spectroscopy in the early 1960s. The excellent energy resolution and good efficiency achieved by these detectors provided experimenters with unprecedented capabilities in gamma-ray measurements, and this has revolutionized the field of gamma-ray spectroscopy. In the 1970s, high-purity Ge became available and rapidly replaced Ge (Li). With high-purity Ge, the detectors are stable at room temperature, and thus the fabrication of detectors can be carried out without the severe time constraints that existed when working with Ge (Li) detectors. This opened up new possibilities in terms of detector processing, and allowed the production of more diverse types of detectors and multi-detector systems.

In the ensuing decades, there have been continuing advances in semiconductor gamma - ray detector technology. Ge detectors continue to increase in size and complexity. More recently, detectors based on other materials, such as Si and CdZnTe, have also been actively developed for gamma-ray detection. Advances in the technology of semiconductor gamma-ray detectors are the results of contributions from many groups.

3.2.1 High-purity Ge detectors

Germanium semiconductor detectors were first introduced in 1962 (Tavendale and Ewan, 1963) and are now the detectors of choice for high energy-resolution γ-ray studies. These detectors directly collect the charges produced by the ionization of the semiconductor material. One electron-hole pair is produced on the average for every 3 eV absorbed from the radiation. These pairs drift under an external electric field to the electrodes where they generate the pulse. The high number of information carriers leads to a small percentage fluctuation and this is the reason for the high energy-resolution of Ge detectors [24]**.** In detection process, production of a pulse whose amplitude is proportional to the energy deposited in the detector.

By far the most common type of application for Ge detectors is basic gamma-ray spectroscopy, where a single detector is used with a single channel of electronics to provide energy information. With modern low-noise electronics and Ge materials, the best energy resolution achieved with Ge detectors at gamma-ray energies is close to the fundamental limits imposed by charge generation statistics. Therefore, further significant improvement in energy resolution is not expected, unless other non-ionization type detection techniques are used. On the other hand, the efficiency of Ge detectors has increased steadily over time. The graph in Fig.3.4a shows how the maximum volume of high-purity Ge detectors increases with time. It is interesting to note that the detector size seems to increase roughly linearly with time. If this trend continues, we will see detectors with volume of 1-liter in a few years!

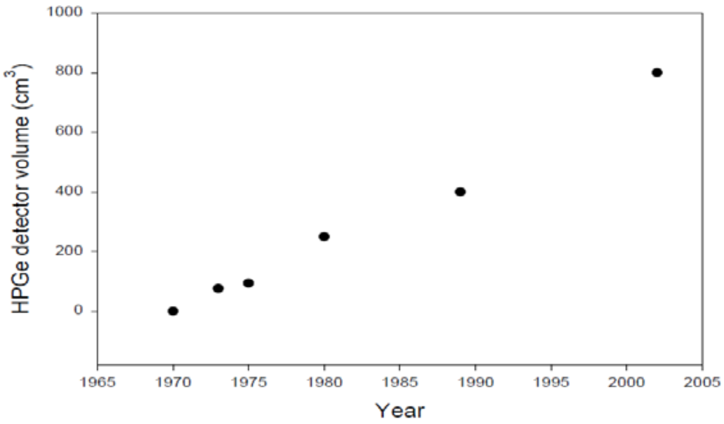

Figure 3.4a: volume of high-purity Ge detectors [29].

Besides increased detector volume, more complex detector structures have been developed to provide additional capabilities such as gamma-ray imaging.

The most basic components of a gamma spectroscopy system are detector (and high voltage power supply) and Multichannel analyzer (MCA). Experimental set up of HPGe detector with associated electronics were arranged according to the Fig. 3.4b shown below [29]**.** The two most important characteristics of HPGe detector are its ***resolution*** and ***efficiency***. Other characteristics to consider are peak shape, peak-to-Compton ratio, pulse rise time, crystal dimensions or shape, and price. The detector's resolution is a measure of its ability to separate closely spaced peaks in the spectrum, and, in general, the resolution is specified in terms of the full width at half maximum (FWHM) of the 122 keV photopeak of ^{57}Co and the 1,332 keV photopeak of ^{60}Co.

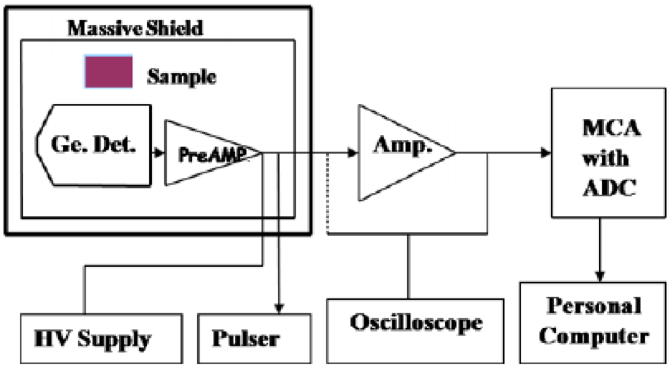

Figure 3.4b: Electronic block diagram of high resolution γ-ray spectrometry system [27].

Analog-digital converter (ADC) is conversion of the analog signal into a digital value. ***Multichannel analyzer (MCA)*** is the recording of the events received in a memory. Spectrometry software is used for piloting of the spectrum acquisition, visualization and processing.

Two "Functions" of the MCA:

1. Count the pulses from the detector. The ***number of pulses*** can be related to the ***activity*** of the radionuclides in the sample (gamma spectrometry).
2. Measure the size of the pulses (pulse height analysis). The ***height of the pulses*** can be related to the ***energy*** of the gamma rays. This is used to identify the radionuclides in the sample.

The amplifier increases the size of the pulses by a factor called the "gain." The gain determines the range of gamma ray energies that are seen on the spectrum. For example, a particular gain might result in a spectrum viewing gamma rays of 20 to 2000 keV [27].

3.2.2 CdZnTe detectors

The use of CdZnTe (Cadmium zinc telluride) crystals as gamma ray detectors started around 1991.CdZnTe is a high Z, wide band gap semiconductor. The wide band gap of CdZnTe allows detectors to operate at room temperature with low leakage currents. In addition, the average Z of CdZnTe is significantly higher than that of Ge, which could potentially yield higher photo peak efficiency. These features make CdZnTe extremely attractive as a gamma-ray detector material. Recently, significant progress has been made in growing large single-crystal CdZnTe for detector fabrication [30].

Our group has focused our effort on the development of a different technique called the "coplanar-grid". The coplanar-grid technique utilizes two interdigital coplanar grid electrodes to sense the motion of charge carriers in the detector. A coplanar-grid CdZnTe detector and the readout scheme are depicted in Fig.3.5. During operation, a high voltage ($-V_b$) is applied to the cathode to sweep carriers across the detector, and a small voltage (V_g) is applied between the two grids to direct the electrons towards one of the grids (collecting grid) and away from the other (non-collecting grid).

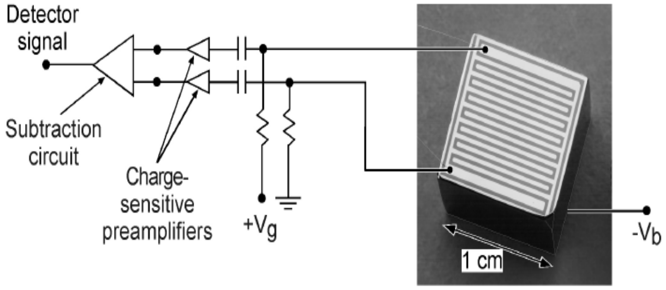

Figure 3.5: A coplanar-grid CdZnTe detector [30].

The signals induced on these two grids by the movement of carriers are subtracted to give a net output signal. This signal can then be processed the same way as that of a conventional detector to perform spectroscopy. This differential signal measurement produces a detector signal that is predominantly determined by the number of electrons reaching the collecting grid. The problem of poor hole collection is then largely eliminated.

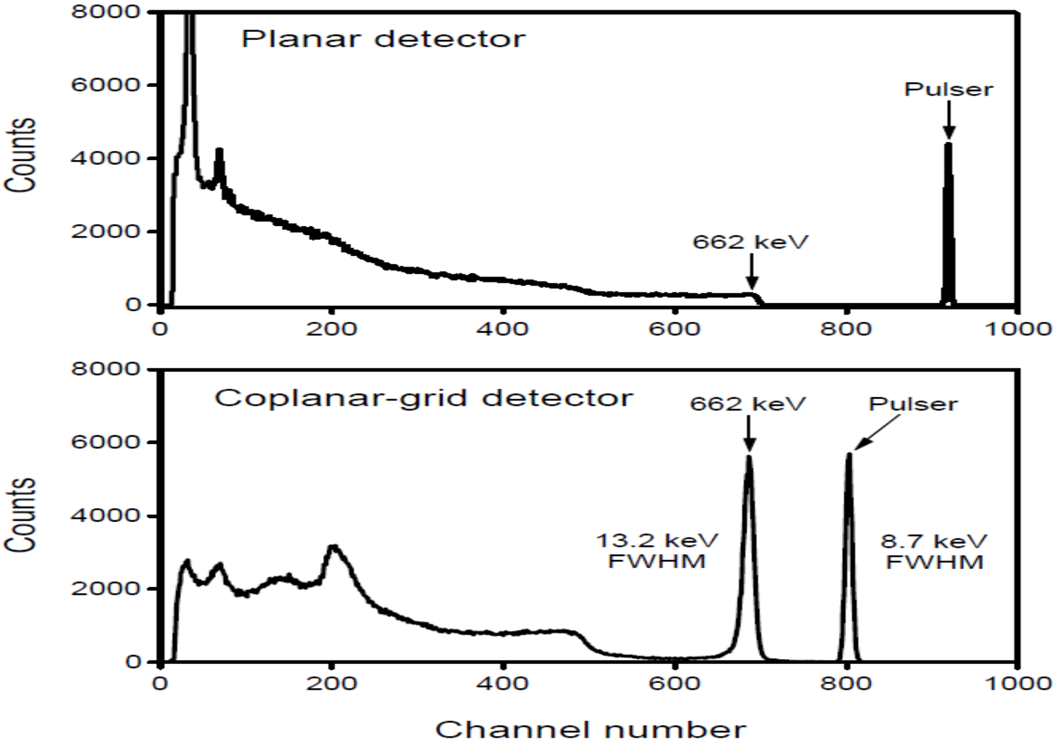

Figure 3.6: The coplanar-grid technique for a 1 cm^3 CdZnTe detector [34].

In addition, by adjusting the relative gain of the two grid signals before subtraction, the effects of electron trapping can be nearly perfectly compensated for [31]**.** The net result is that the detector signals become independent of the depths of gamma-ray interactions over much of the detector volume, and therefore excellent energy resolution can be obtained. Fig. 3.6 shows the very large improvement in spectral response that is achieved using the coplanar-grid technique for a 1 cm^3 CdZnTe detector. Although the energy resolution is still significantly worse than Ge, it is several times better than that of scintillation detectors. With the coplanar-grid technique, it is theoretically possible to achieve resolution close to that of Ge detectors given the typical carrier lifetime already achieved with present CdZnTe materials. The two main factors that are now limiting the energy resolution are material non-uniformity and electronic noise. Progress is being made in understanding these problems and to further improve detector performance.

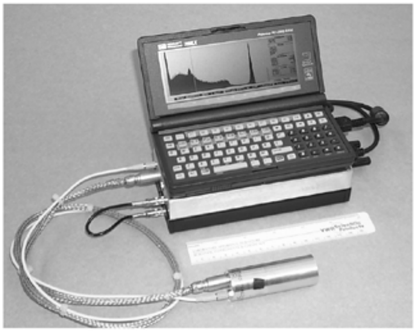

Figure 3.7: shows a photograph of a prototype portable detection system [30].

The ability of CdZnTe detectors to operate at room temperature and the simplicity of electronics required to implement the coplanar-grid technique make it possible to build highly compact detection systems.

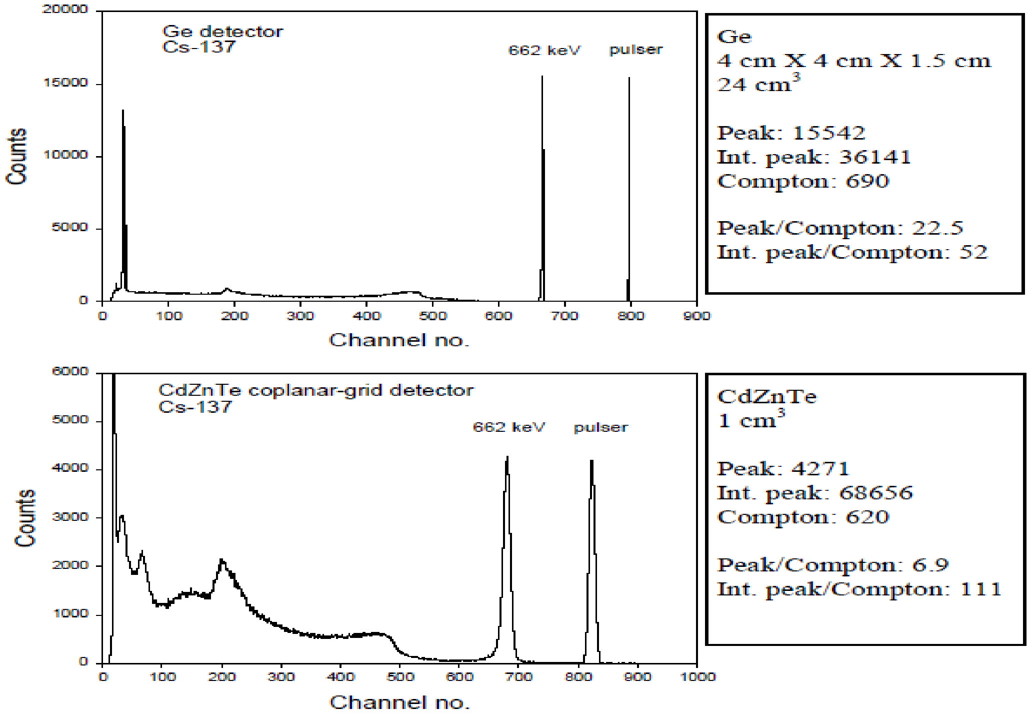

Figure 3.8: A comparison of ^{137}Cs spectra obtained from a 24 cm^3 Ge detector and a 1 cm^3 CdZnTe coplanar-grid detector [33].

Fig.3.7 shows a photograph of a prototype portable detection system we have assembled using a 1 cm^3 coplanar-grid CdZnTe detector and a commercial multi-channel analyzer (MCA). A much more compact system, containing a 2 cm^3 detector, is currently being developed. Despite the relatively small volume of these detectors at the present time, the detection efficiency is quite good due to the high Z of CdZnTe. As an illustration, Fig.3.8 shows a comparison of ^{137}Cs spectra obtained from a 24 cm^3 Ge detector and a 1 cm^3 CdZnTe coplanar-grid detector [31]. The spectra were taken with different source-to-detector distances so absolute efficiency comparison cannot be made, but valid comparisons can be made using peak-to-Compton ratios. The Ge detector has a higher peak-to-Compton ratio as normally defined, but this is mainly due to its much better energy resolution. If the integrated photo peak counts are used to compute an "integrated photo peak"-to-Compton ratio, the CdZnTe detector is twice more efficient in capturing the full energy of the gamma rays than the Ge detector, even though the Ge detector has 1.5 times the thickness and 24-times the volume [30].

3.3 Detector efficiency

Generally, the sensitivity of HPGe system will be in direct proportion to the detector efficiency. The efficiency of a detector is a measure of how many pulses occurs for a given number of gamma rays, i.e., the fraction of all the photons that are emitted by the source or sample (A), which cause an event in the detector (N). This is the efficiency ε of that detector.

$$N = \varepsilon .\ A$$

Detector efficiency for a given detector depends on gamma-ray energy and the sample and detector geometry, i.e. subtended solid angle. Of course, a larger volume detector will have a higher efficiency.

Total efficiency (ε_{tot}***)*** is the ratio of total number of detected photons in the full-energy peak to the total number of photons emitted by the source.

Various kinds of efficiency definitions are in common use for gamma-ray detectors. They are given below:

a. ***Absolute Efficiency*****:** The ratio of the number of counts produced by the detector to the number of gamma rays emitted by the source (in all directions).

b. ***Intrinsic Efficiency:*** The ratio of the number of pulses produced by the detector to the number of gamma rays striking the detector. The intrinsic efficiency of a detector is defined in terms of the number of photons in a collimated beam incident on its entrance window; and not by the number of photons emitted by the source. This definition has the advantage that it is not tied to any source-detector geometry. It is often used to compare different detectors; but is of little importance when measuring the activity of radioactive samples [38].

c. ***Relative Efficiency:*** Relative to NaI it is common practice to specify the efficiency of a HPGe detector at 1332 keV (^{60}Co) as a percent of the efficiency of a 3 in. by 3 in. NaI detector at 25-cm source-to-detector distance and the same gamma-ray energy:

$$\boldsymbol{\varepsilon_{rel}\ \text{to NaI (Ge)} = 100\ \varepsilon_{tot}(\text{Ge, 1332 keV})/\varepsilon_{tot}\ (\text{NaI, 1332 keV})\ .}$$

The theoretical value of ε_{tot}(NaI, 1332 keV) at 25 cm is 1.2×10^{-3}. Thus, for example, a 30% (relative) germanium detector has a theoretical absolute efficiency at 1332 keV at 25 cm of 3.6×10^{-4} [32].

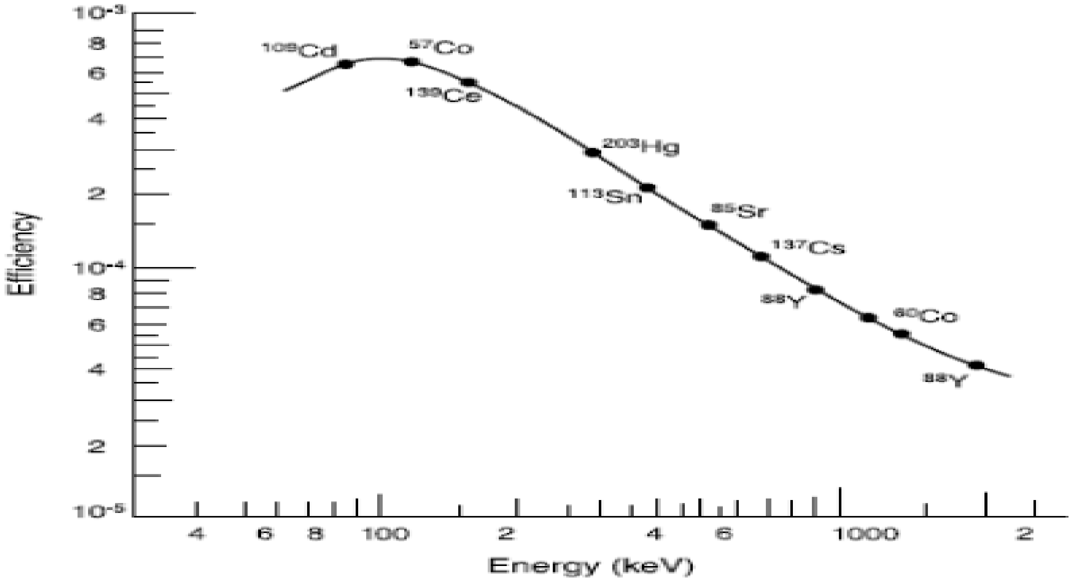

Figure 3.9: Full-energy peak efficiency curve for a germanium detector [35].

d. ***Full-Energy Peak (or Photopeak) Efficiency:*** The efficiency for producing full energy peak pulses only, rather than a pulse Efficiency curve of any size for the gamma-ray. It is clear from the previous discussion that the photopeak efficiency of a detector will be dependent on the energy of the photon interacting with it.

Clearly, to be useful, the detector must be capable of absorbing a large fraction of the gamma-ray energy. This is accomplished by using a detector of suitable size, or by choosing a detector material of suitable high Z. Detectors of greater than 100% relative efficiency have been fabricated from germanium crystals ranging up to about 75 mm in diameter. About two kg of germanium is required for such a detector. An example of a full-energy peak efficiency curve for a germanium detector is shown in Figure 3.9

3.4 Detector resolution

The width of the peaks is determined by the resolution of the detector, a very important characteristic of gamma spectroscopic detectors, and high resolution enables the spectroscopist to separate two gamma lines that are close to each other. Gamma spectroscopy systems are designed and adjusted to produce symmetrical peaks of the best possible resolution. The peak shape is usually a Gaussian distribution. In most spectra the horizontal position of the peak is determined by the gamma-ray's energy, and the area of the peak is determined by the intensity of the gamma-ray the efficiency of the detector.

Resolution is a measure of the width (full width at half max, FWHM) of a single energy peak at a specific energy, either expressed in absolute keV (as with Germanium Detectors), or as a percentage of the energy at that point (Sodium Iodide Detectors). Figure 3.10 shows calculation of FWHM energy resolution.

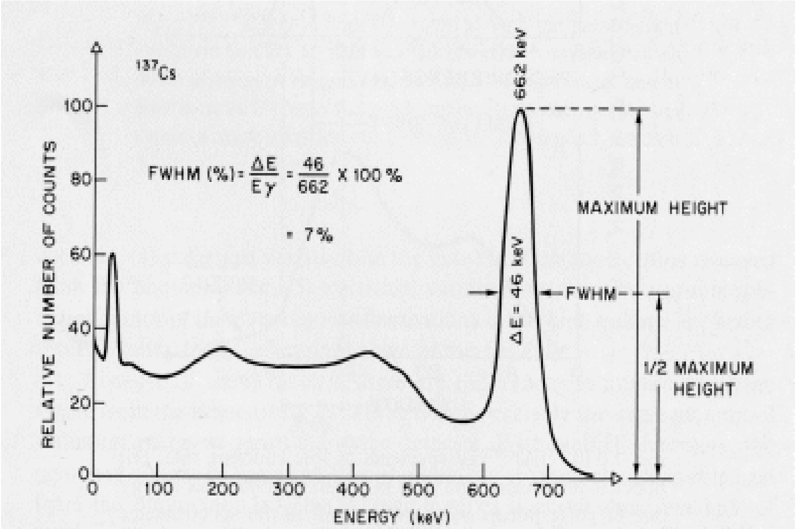

Figure 3.10: calculation of FWHM energy resolution of a NaI (TI) detector for ^{137}Cs 662 keV γ rays [37].

One of the measurement methods in scintillation counting is the spectrum method that uses a pulse height analyzer to measure an energy spectrum. In the spectrum method, pulse height discrimination is very important to determine the photoelectric peaks produced by various types of radiation. This is evaluated as "energy resolution" or "pulse height resolution (PHR)".

Energy resolution is defined by the following equation. It is generally expressed as a percent:

$$R=\Delta P/P,$$

where R is energy resolution, P is peak value (E_0), and ΔP is FWHM.

As a general rule, semi-conductors (Ge) enable better spectrum resolution than scintillators (NaI). A NaI(Tl) detector has an energy resolution of only about 10%. [More advanced detectors such as high purity germanium detectors have as much as 30 times greater resolution, but are much more expensive [37].] There are three factors that give germanium the excellent resolution that it has: the inherent statistical spread in the number of charge carriers, variations in the charge collection efficiency, and contributions of electronic noise [36]. Some of these factors will dominate over the other factors, but this is dependent on the energy of the radiation and the size and quality of the detector in use.

When a beam of mono-energetic gamma-rays strikes the scintillator, there is a fluctuation from gamma-ray to gamma-ray in the height of the voltage pulse from the photomultiplier, which shows up as a broadening of the photopeak. The pulse height variation is chiefly due to statistical fluctuations in the number of electrons emitted at the cathode of the photomultiplier when a flash of photons arrives from the scintillator, but is also due to the occasional escape of electrons, X-rays or gamma-rays from the crystal, all of which depend on how large the NaI crystal is. The full width of a peak at half its maximum height (FWHM) is a convenient measure of the resolution of the instrument. A high energy resolution means that the detector can discriminate between gamma-rays with similar energies. The more resolution a detector has, the more defined a gamma spectrum becomes.

The resolution of a scintillator (e.g., NaI) specified for the 662 keV gamma ray of Cs-137 is 7-8%.

$$\text{Energy resolution} = 100 \times (E_2 - E_1)/E_0,$$

where E_2 - E_1 is the full width half maximum (FWHM) and E_0 is 662 keV.

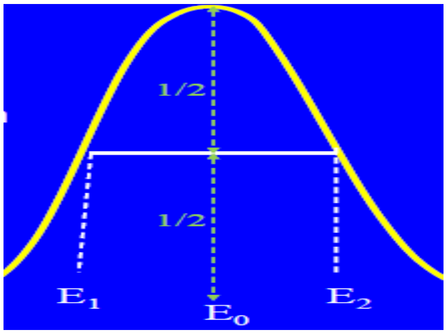

3.11: The resolution of a scintillator (e.g., NaI or HPGe) [36].

The resolution of a HPGe detector is usually specified as the FWHM (in keV) for the 1332.5 keV peak of Co-60. Typical resolutions are 1.7 – 2.0 keV.

The narrower the peaks, the better the resolution. Narrower peaks (better resolution) mean a greater ability to distinguish gamma rays of similar energies.

Chapter 4

Gamma ray Spectrometry

Gamma Spectrometry refers to the process of using the number of emitted gamma-rays to quantify the activity of the radionuclides. For more than 50 years, gamma-ray spectrometry has been used to map rocks/soils, find hydrocarbon and mineral deposits/mines, monitor environmental hazards, and detect radioactive sources [40].

4.1 Analysis of natural gamma-ray spectra

Natural gamma-ray (NGR) spectrometry allows estimation of the elemental concentrations of Potassium, Uranium, and Thorium which can be used to help interpret sediment composition, provenance, and diagenesis. Spectral data obtained with the NGR multichannel device installed on the Ocean Drilling Program's multisensor track in 1993 are presented here for the first time. The spectra were divided into 16 energy intervals using a minima search algorithm that defined all peaks observed in 79 sample NGR spectra.

The intervals were further subdivided into peak area and background area segments using a peak baseline algorithm, which allows optimal assessment of the usefulness of spectral segments to estimate elemental abundance [41]. Linear regression with laboratory (X-ray diffraction, inductively coupled plasma-mass spectrometry, and instrumental neutron activation analyses) data was used to estimate elemental concentrations of K, U, and Th for each spectral segment. Conservative estimation errors for the best estimator spectral segments are 16%, 30%, and 20% for K, U, and Th, respectively. These errors also reflect analytical errors of the reference data, and the true estimation error may be significantly smaller. Our method suggests that the best K estimates (± 16%) are obtained using the peak area segment between 1335 and 1580 KeV. In our study, which uses 4-hr counting times, the best U and Th estimates are obtained using peak areas between 1695 and 1885 KeV and 550 and 700 KeV, respectively.

If low counting times are used for routine core logging, however, regressions using the total counts of the entire spectrum yield more reliable U and Th estimates because of Poisson's law, with maximum total errors of about 35% and 23%, respectively. Spectral analysis using 2048-channel data has no advantage over 256-channel analyses, even with the extremely high counting times used for our study. The full character of natural gamma-ray spectra, as revealed by scintillation detectors, can be defined and measured in full detail with 16 energy intervals. Natural gamma-ray (NGR) spectrometry allows estimation of elemental concentrations of Potassium, Uranium, and Thorium through the gamma emission of their radioactive isotopes ^{40}K, the ^{238}U series, and the ^{232}Th series. These most important “primeval” natural gamma-ray emitters are at secular equilibrium with their parent elements (i.e., radiation at characteristic energies is constant with time; Adams and Gaspirini, 1970). The relative abundance of K, U, and Th estimated from well-logging data has been shown to help characterize clay type and abundance, depositional environment, and diagenetic processes in sediments (Serra et al., 1980; Serra, 1984, 1986).

Because NGR spectrometry provides rapid, continuous, and inexpensive lithological parameters in geological formation testing, we explored its adaptation to the routine continuous core logging of the Ocean Drilling Program (ODP). An NGR measurement device was installed by the ODP on the *JOIDES Resolution* in 1993 as part of the multisensor track (MST) for continuous core logging. General energy calibration, measurement, and correction procedures were introduced by Hoppie et al. (1994). The original intent for the instrument was to measure total counts to aid correlation of core and down hole geophysical data. However, the device is equipped with a 2048-channel multichannel analyzer and adequate software to allow spectral data acquisition. ODP had introduced the five-window spectral data acquisition used by its down hole measurement contractor, Schlumberger Services, to provide the scientists with a standard spectral data set, but no absolute calibration standards, model spectra, or estimation algorithms exist to estimate elemental concentrations.

NGR spectra of rocks and soils are composed of one emission peak of ^{40}K, more than a dozen emission peaks of the ^{238}U series (mainly ^{214}Bi), a similar number of ^{232}Th peaks (^{208}Tl, ^{228}Ac), and total background. Total background originates from two completely different sources. Zero-background is the combination of cosmic radiation, impurities in detector crystal, and contamination in the measurement system (e.g., soil deposits inside the lead shielding), and is unrelated to the composition of the measured material [42]. It is determined separately and removed from core spectra before spectral analysis (Fig. 4.1). What we will refer to as background from here on is produced by Compton scattering, photoelectric absorption, and pair production related to the abundance and distribution of primeval emitters, as well as by low-intensity, discrete emission peaks of U and Th, which disappear in the scatter.

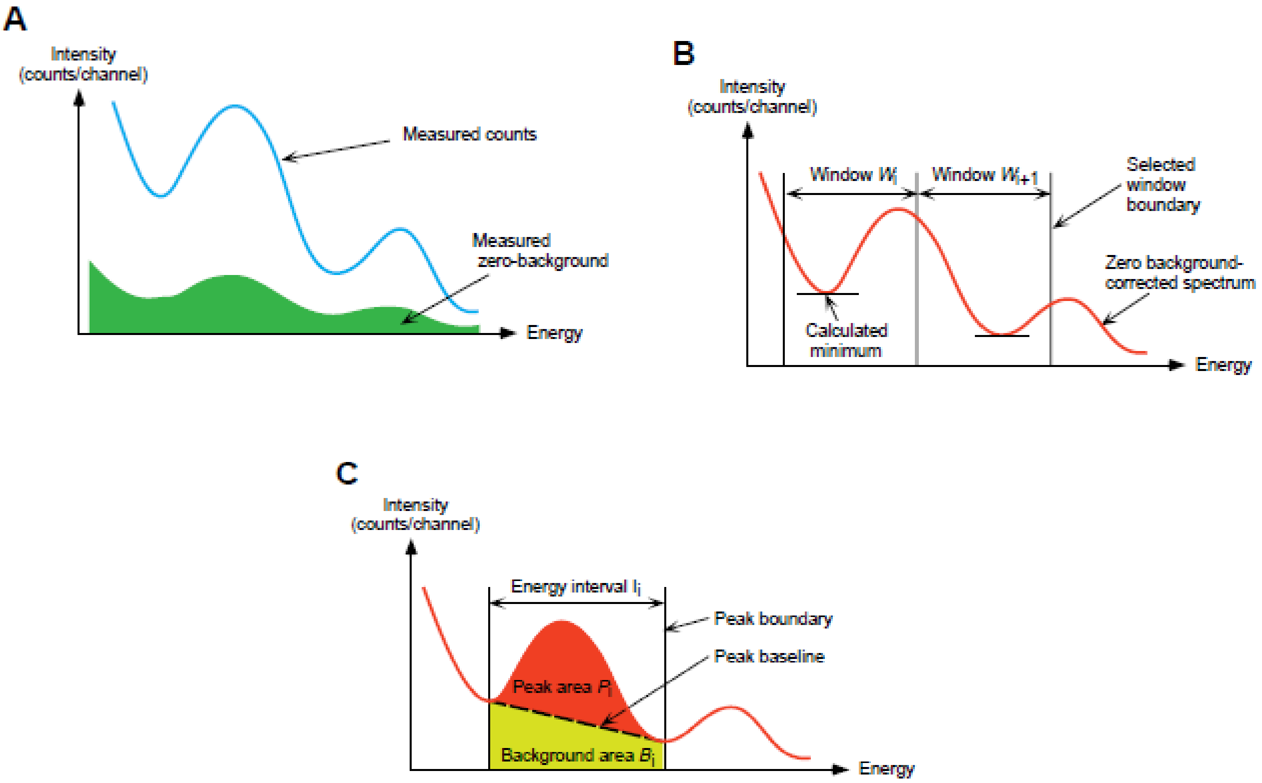

Figure 4.1. Schematic portion of a natural gamma-ray (NGR) spectrum illustrating the peak definition procedure. A Zero-background, including cosmic radiation, impurities in sensor, and contamination in measurement area, is measured separately and subtracted from measured counts of sample spectra. B. In the zero-background–corrected spectrum, window boundaries are selected near energies of characteristic peaks identified from typical sample spectra. Minima are then calculated within each window for each sample spectrum. C. Peak baseline is defined by two adjacent minima and separates the integrated count area into peak area and background area [45].

Background, as well as limited detector efficiency degrades NGR spectra; only a few peaks are discernible as individual bell-shaped peak areas above background (Figs. 4. 1). In fact, the main, characteristic peaks above background for the three elements only comprise a few percent of the total counts of the entire spectrum. Using only these characteristic peaks may result in severe statistical counting errors at reasonable counting times. Therefore, the common method applied by commercial well-logging services and airborne surveys is to include background in a simple three-standard calibration procedure under the assumptions that background in a given energy interval varies linearly with the abundance of the three elements, and that this relationship holds for all element distributions encountered. Elemental concentrations are then estimated using the method of weighted least squares, where the counts vector is the product of the sensitivity matrix and the concentration vector. The International Atomic Energy Agency (1976) suggests that K, U, and Th concentrations are calculated from counts in three discrete windows defined narrowly around the three main characteristic peaks. Mathis et al. (1984) presented a window stripping and calibration study for the spectral gamma-ray (SGR) tool of Gearhart Services, which is based on 256 channels and provides either a routine three window analysis or the raw spectra to the customer. For all these tools, elemental abundance is calculated using a sensitivity matrix obtained from segments of known concentrations of K, U, and Th in a calibration well.

Because the ODP system is not equipped with absolute calibration standards, we extracted core samples from the intervals measured with the ODP NGR device and determined reference concentrations in shore laboratories. We used linear regression to evaluate particular segments of the spectrum for their significance as elemental concentration estimators. The NGR spectra were measured for 4 hr to minimize counting errors, which was possible during Leg 156 because most of the time was expended for extensive down hole operations rather than for coring, allowing us to run an unusual number of dedicated NGR spectral measurements on idle instrumentation [44].

4.2 Calculation of the Peak Areas of Phootpeaks

The area of a peak is the difference between its entire area and the respective background. The background comprises all pulses that do not belong to the photopeak but have been registered by the multichannel analyzer in the channels of the peak. The main reasons for the background are:

- Natural radiation at the place of measurement (e.g. cosmic radiation, terrestrial radiation),
- Artificial radiation at the place of measurement (e.g. operation of the reactor, storage of radiation sources close to the place of measurement)
- Background of Compton scattering originating from higher gamma energies of the sample being analyzed.

The first two components of the background can be minimized by shielding the gamma detector (e.g. with lead) and/or by storing other gamma sources as far as possible from the place of measurement. If the sample being analyzed has more than one gamma line, the third background component is often dominating and cannot be avoided.

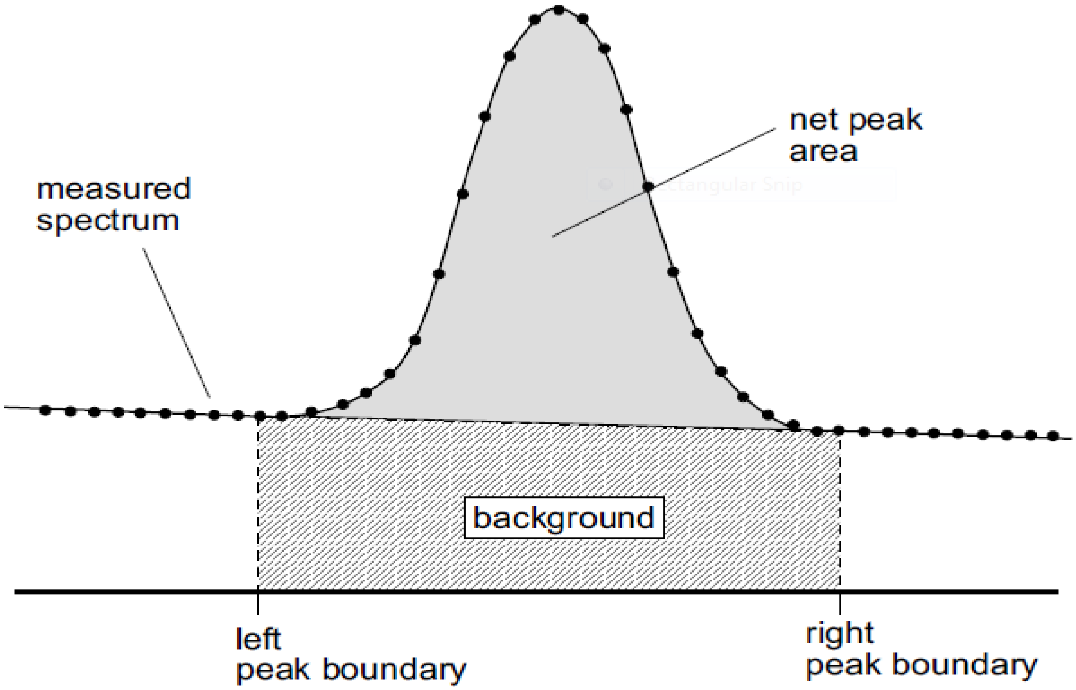

Figure.4.2.Principle of net peak area determination [45].

For correcting the background, the "ceiling" is assumed to have a linear shape (see Fig. 4.2.). In this case, it can be written

$$B = \left(\frac{C_1 + C_n}{2}\right) \cdot n \tag{4.1}$$

$$A_g = \sum_{i=1}^{n} C_i \tag{4.2}$$

$$A_n = A_g - B = \sum_{i=1}^{n} C_i - \left(\frac{C_1 + C_n}{2}\right) \cdot n \tag{4.3}$$

where B is area of the background, A_g is gross peak area, A_n is net peak area, C_1 is content of the channel at the left boundary of the peak, C_i is content of the i-th channel, C_n is content of the channel at the right boundary of the peak, and n is number of channels between left and right boundaries.

The software of the multichannel analyzer can calculate automatically the gross and net peak areas as well as the respective standard deviations, which are due to the counting statistics.

4.3 Calculation of elemental concentrations (Absolute method)

The Laboratory equipment includes a semiconductor detector HPGe (Canberra GX4020) with the resolution 1.9 keV (for the line 1333 MeV), energy range above 3 keV and relative efficiency 42%. The detector is supported by an integrated spectrometric setup Desktop InSpector (Canberra). The electronic setup is paired with a computer with an original data acquisition and the processing Genie 2000 software (Canberra), responsible for the data analysis and support of the spectrometric setup. During routine measurements, the detector is covered with hood-shaped protection cap made of polyethylene, 1.4 mm in thickness, over the detector window [42].

The detector is placed in a housing made of lead bricks, with a 1 mm cadmium and 1 mm copper inner lining; the upper and side walls are 10 cm in thickness, the bottom wall is 15 cm thick. The upper cover is mobile, which enables an easy replacement of samples.

Depending on their type and accessibility, environmental samples vary in volume from several to several hundred cm^3. In order to optimize the measurement procedure, 3 geometries are used: the Marinelli beaker – a vessel of 710 cm^3 (20 mm layer of material surrounding the detector) and cylindrical geometries: 121.2 cm^3 (sample diameter 70 mm, height 31.5 mm) and 48.4 cm^3 (sample diameter 70 mm, height 12.5 mm). The samples are placed in aluminum vessels with walls 1 mm thick and positioned directly on the detector. The methodology outlined below applies to the cylindrical geometry 121.2 cm^3 [43]. As regards other geometries, the methodology is the same. The solid material to be measured is ground below 0.5 mm, then dried to constant mass, placed in a vessel and covered with an aluminum lid. In measurements of concentration of some natural radionuclides the daughters of radon are determined, e.g. Bi-214, Ac-228, to prevent radon escape from the sample the lid-vessel connection is sealed with a gas-proof butyl compound. The sample should be sealed for about 3 weeks prior to measurements, in order to achieve the radioactivity equilibrium [43].

The duration of routine measurements is so chosen that the relative uncertainty of the counts number for the lines used in nuclide concentration calculations should be less than 5%. This time depends on the concentration of analyzed nuclides and typically ranges from 10 h to about 50 h (for Marinelli geometry from several hours to about 20 h, respectively) [44].

Following the spectrum analysis, count rates for each detected photopeak and activity per mass unit (specific activity or radiological concentration) for each of the detected nuclides are calculated. The specific activity (in *Bq kg−1*), A_{Ei} , of a nuclide *i* and for a peak at energy *E*, is given by:

$$A_{Ei} = \frac{N_{Ei}}{\varepsilon_E \times \ t \times \gamma_d \times M_s} \tag{4.4}$$

where N_{Ei} is the Net Peak Area of a peak at energy *E*, ε_E is the detection efficiency at energy *E*, *t* is the counting live time, γ_d is the number of gammas per disintegration of this nuclide for a transition at energy *E*, and M_s is the mass in *kg* of the measured sample. If there is more than one peak in the energy analysis range for a nuclide, then an attempt to average the peak activities is made. The result is then the weighted average nuclide activity [48]. Based on the measured γ-ray photopeaks, emitted by specific radionuclides in the ^{232}Th and ^{238}U decay series and in ^{40}K, their radiological concentrations in samples collected were determined. Calculations relied on establishment of secular equilibrium in the samples, due to the much smaller lifetime of daughter radionuclides in the decay series of ^{232}Th and ^{238}U. More specifically, the ^{232}Th concentration was determined from the average concentrations of ^{212}Pb and ^{228}Ac in the samples, and that of ^{238}U was determined from the average concentrations of the ^{214}Pb and ^{214}Bi decay products. Thus, an accurate measurement of ^{232}Th and ^{238}U radiological concentrations was made, whereas a true measurement of ^{40}K concentration was achieved [46].

Radiological concentrations of ^{232}Th, ^{238}U and ^{40}K were then converted into total elemental concentrations of thorium, uranium and potassium, respectively, according to the following expression:

$$F_E = \frac{M_E \cdot C}{\lambda_E \cdot N_A \cdot f_{A,E}} \cdot \frac{1}{n} \sum_{i=1}^{n} A_i \tag{4.5}$$

where F_E is the fraction of element *E* in the sample, M_E is the atomic mass *(kg mol^{-1})*, λ_E is the decay constant *(s^{-1})* of the parent radioisotope, N_A is Avogadro's number (6.023×1023 *atoms mol^{-1}*), $f_{A,E}$ is the fractional atomic abundance of ^{232}Th, ^{238}U or ^{40}K in nature, *C* is a constant (with a value of 100 or 1,000,000) that converts the ratio of the element's mass to soil mass into a percentage or *ppm*, and A_i is the radiological concentration of ^{40}K (n=1) or that of selected daughter radionuclides in the decay series of ^{232}Th and ^{238}U (n=2). Total elemental concentrations are reported in units of parts per million (*ppm*) for thorium and uranium, and of percent (%) for potassium.

4.4 Calculation of concentration by other methods

Comparison method: The activity concentration of the radionuclides in the samples was calculated using the comparison method, given by the equation

$$\frac{C_r M_r}{I_r} = \frac{C_s M_s}{I_s}, \tag{4.6}$$

where C_r is the radionuclide activity concentration in the standard reference sample, M_r is the mass of standard reference sample, I_r is the peak intensity of the radionuclide in the standard sample, C_s is the activity of radionuclide in the sample, M_s is the mass of the sample and I_s is the peak intensity of the radionuclide in the sample [47].

Chapter 5

Application of Gamma ray spectroscopy

5.1 Medical Application

Nuclear medicine is a medical specialty that uses radioactive tracers (radiopharmaceuticals) to assess bodily functions and to diagnose and treat disease. Specially designed cameras allow doctors to track the path of these radioactive tracers. Single Photon Emission Computed Tomography or SPECT and Positron Emission Tomography or PET scans are the two most common imaging modalities in nuclear medicine [49]. Nuclear medicine imaging uses small amounts of radioactive materials called radiotracers that are typically injected into the bloodstream, inhaled or swallowed. The radiotracer travels through the area being examined and gives off energy in the form of gamma-rays which are detected by a special camera and a computer to create images of the inside of your body [50]. Nuclear medicine imaging provides unique information that often cannot be obtained using other imaging procedures.

Nuclear medicine is a branch of medical imaging that uses small amounts of radioactive material to diagnose and determine the severity of or treat a variety of diseases, including many types of cancers, heart disease, gastrointestinal, endocrine, neurological disorders and other abnormalities within the body. Because nuclear medicine procedures are able to pinpoint molecular activity within the body, they offer the potential to identify disease in its earliest stages as well as a patient’s immediate response to therapeutic interventions.

Nuclear medicine imaging procedures are noninvasive and, with the exception of intravenous injections, are usually painless medical tests that help physicians diagnose and evaluate medical conditions. These imaging scans use radioactive materials called radiopharmaceuticals or radiotracers. Depending on the type of nuclear medicine exam, the radiotracer is either injected into the body, swallowed or inhaled as a gas and eventually accumulates in the organ or area of the body being examined. Radioactive emissions from the radiotracer are detected by a special camera or imaging device that produces pictures and provides molecular information [51].

Physicians use radionuclide imaging procedures to visualize the structure and function of an organ, tissue, bone or system within the body.

In many centers, nuclear medicine images can be superimposed with computed tomography (CT) or magnetic resonance imaging (MRI) to produce special views, a practice known as image fusion or co-registration. These views allow the information from two different exams to be correlated and interpreted on one image, leading to more precise information and accurate diagnoses. In addition, manufacturers are now making single photon emission computed tomography/computed tomography (SPECT/CT) and positron emission tomography/computed tomography (PET/CT) units that are able to perform both imaging exams at the same time. An emerging imaging technology, but not readily available at this time is PET/MRI.

The basic principles of radionuclide imaging are a radioactive substance, usually combined with a biologically active compound, is injected into the patient. This targets a particular organ or tissue type and the radiation emitted is detected and used to form an image of, or the function of, that organ. The most common radioactive substances used emit gamma rays (usually in the energy range 100–300 keV). More than 95 per cent of all gamma camera imaging techniques use technetium-99m (Tc-99m). This radionuclide is particularly useful because it produces only gamma rays (by isomeric transition), the gamma rays have an appropriate energy of 140 keV, the physical half-life of Tc-99m is about 6 hours, so injection and imaging can take place in a reasonable period of time but the patient does not remain radioactive for a long period, and it can readily be combined with biologically active substances to form a variety of radiopharmaceuticals.

Tc-99m is produced by the beta decay of molybdenum-99 by the reaction:

$$^{99}\text{Mo} \rightarrow {}^{99m}\text{Tc} + \text{electron} + \text{neutrino}$$

Nuclear medicine imaging uses safe, painless, and cost effective techniques to image the body and treat disease. It uses very small amounts of radioactive pharmaceuticals and traces their progress through your body. It is unique, because it helps doctors “view” how your body is functioning and its therapy uses larger amounts of radiation to treat thyroid disease and cancer.

Gamma camera overview is shown in Figure 5.1-a below, it can give you a 2D image of the bio-distribution of a radiopharmaceutical. Gamma camera consists parallel hole collimator, large NaI(Tl) crystal, multiple PMTs and position arithmetic circuits. Gamma-camera Principle is shown in Figure 5.1-b below

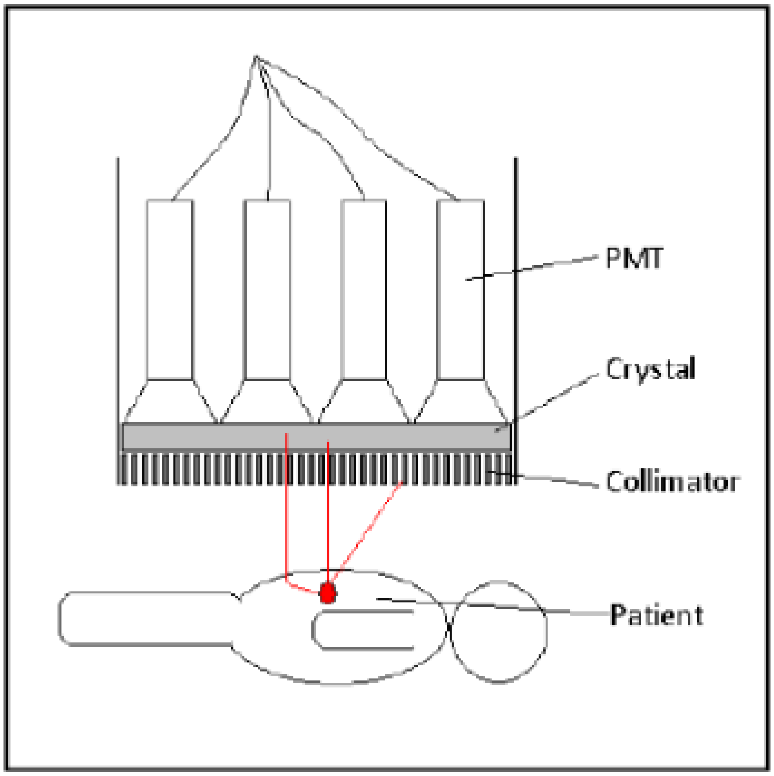

Figure 5.1-a: Gamma Camera Overview [52].

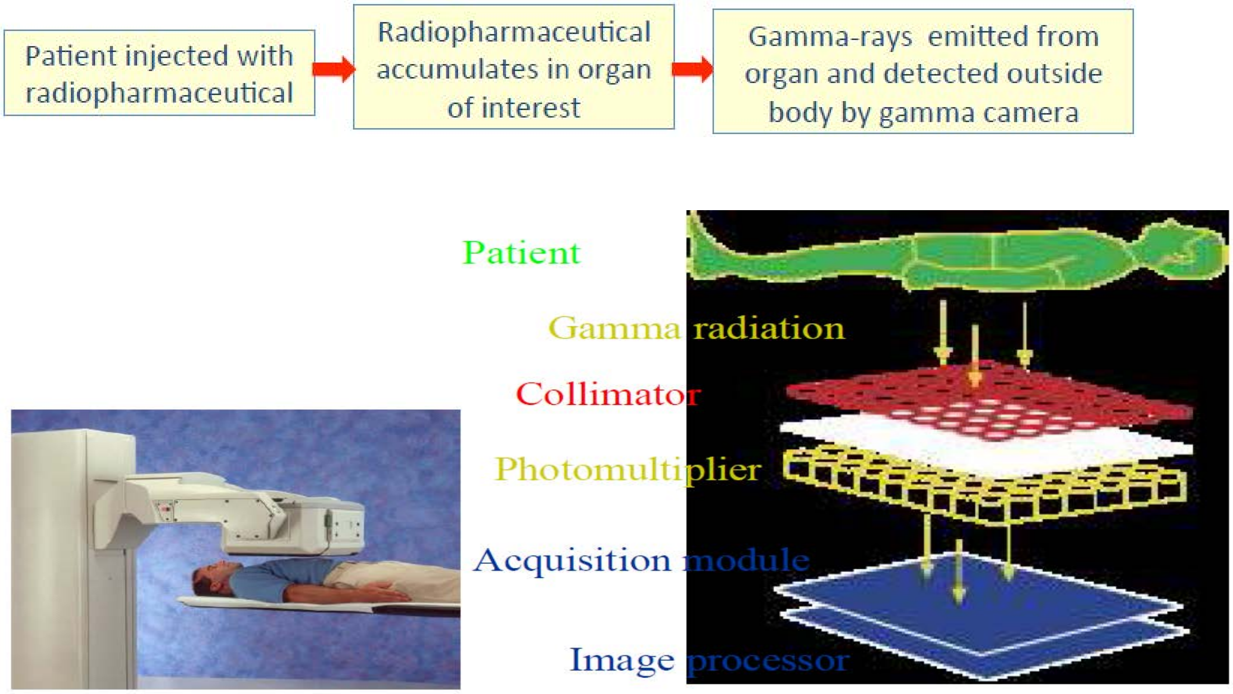

Figure 5.1-b: Gamma-camera Principle [53].

5.1.1 Scintigraphy (nuclear medicine)

Scintigraphy refers to the use of gamma radiation to form images following the injection of various radiopharmaceuticals. The key word to understanding scintigraphy is ‘radiopharmaceutical’. ‘Radio’ refers to the radionuclide, i.e. the emitter of gamma rays. The most commonly used radionuclide in clinical practice is technetium, written in this project paper as ^{99}mTc, where 99 is the atomic mass, and the ‘m’ stands for metastable. Metastable means that the technetium atom has two basic energy states: high and low. As the technetium transforms from the high-energy state to the low-energy state, it emits a quantum of energy in the form of a gamma ray, which has energy of 140 keV (see Fig. 5.2). Other commonly used radionuclides include gallium citrate (^{67}Ga), thallium (^{201}Tl), indium (^{111}In) and iodine (^{131}I). The ‘pharmaceutical’ part of radiopharmaceutical refers to the compound to which the radionuclide is bound. This compound varies depending on the tissue to be examined. For some applications, such as thyroid scanning, free technetium (referred to as pertechnetate) without a binding pharmaceutical is used.

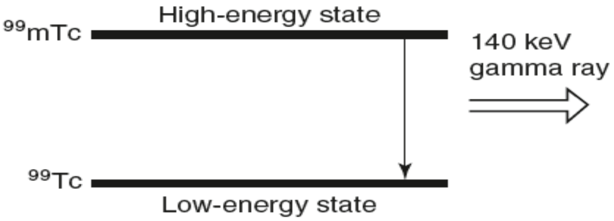

Figure 5.2: Gamma ray production. The metastable atom ^{99}mTc passes from a high-energy to a low-energy state and releases gamma radiation with a peak energy of 140 keV [54].

5.1.2 Single photon emission CT and single photon emission CT–CT

Single photon emission CT (SPECT) is a scintigraphic technique whereby the compute is programmed to analyses data coming from a single depth within the patient. SPECT allows greater sensitivity in the detection of subtle lesions overlain by other active structures (Fig.5.3). The accuracy of SPECT may be further enhanced by fusion with CT. Scanners that combine SPECT with CT are now widely available. SPECT–CT fuses highly sensitive SPECT findings with anatomically accurate CT images, thus improving sensitivity and specificity.

For most diagnostic studies in nuclear medicine, the radioactive tracer is administered to a patient by intravenous injection, but a radioactive tracer may also be administered by inhalation, by oral ingestion, or by direct injection into an organ. The mode of tracer administration will depend on the disease process that is to be studied. The Nuclear Medicine Physician will select the tracer that will provide the most specific and reliable information for a patient's particular problem. The tracer that is used determines whether the patient receives a SPECT or PET scan.

SPECT imaging instruments provide 3 dimensional (tomographic) images of the distribution of radioactive tracer molecules that have been introduced into the patient's body. The 3D image data sets are computer generated from a large number of projection images of the body recorded at different angles. SPECT imagers have gamma camera detectors that can detect the gamma emissions from the isotopes that have been injected into the patient [55]**.** Gamma rays are a form of light that move at a different wavelength than visible light. The cameras are mounted on a rotating gantry that allows the detectors to be moved in a tight circle around a patient who is lying motionless on a palette.

SPECT scans are primarily used to diagnose and track the progression of heart disease, such as blocked coronary arteries. There are also radiotracers to detect disorders in bone, gall bladder disease and intestinal bleeding. Recently SPECT agents have become available for aiding in the correct diagnosis of Parkinson's disease in the brain, and distinguishing this malady from other anatomically-related movement disorders and dementias [55][56].

The main applications of SPECT–CT include ^{99}mTc bone scanning, ^{201}Tl cardiac scanning, ^{99}mTc-MIBG (metaiodobenzylguanidine) staging of neuroblastoma, I-131 MIBG (radioactive iodine labeled with metaiodobenzylguanidine) used to treat adrenal gland tumors in adults and adrenal gland/nerve tissue tumors in children, and Cerebral perfusion studies.

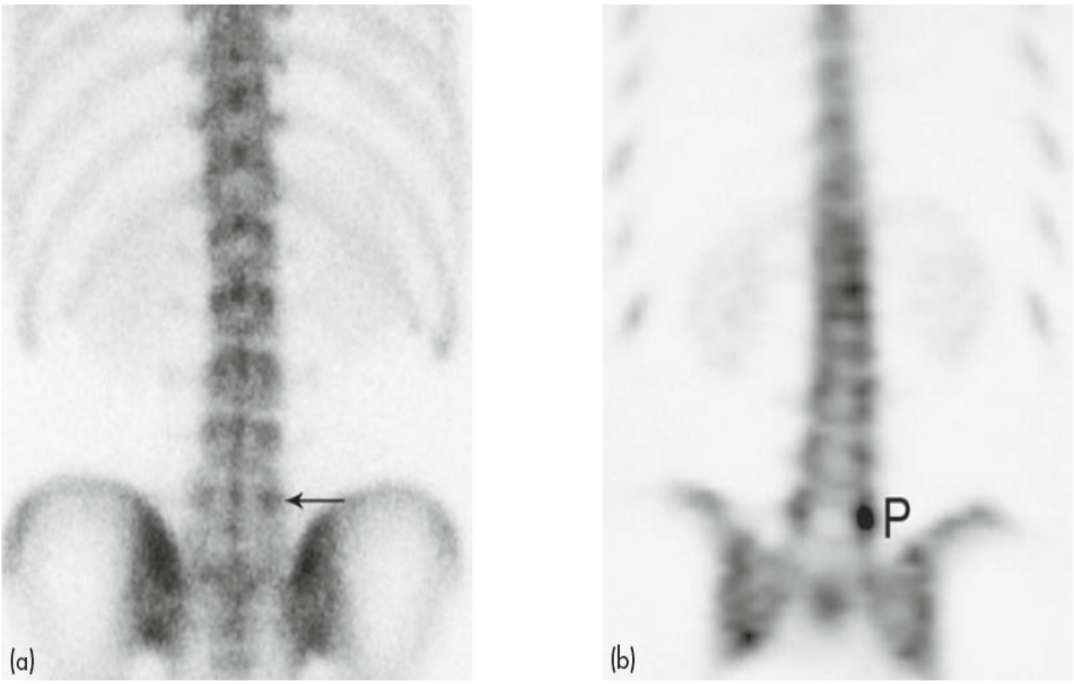

Figure 5.3: Single photon emissions CT (SPECT). (a) Scintigraphy in a man with lower back pain shows a subtle area of mildly increased activity (arrow). (b) SPECT scan in the coronal plane shows an obvious focus of increased activity in a pars interarticularis defect (P) [56].

5.1.3 Positron emission tomography (PET) and positron emission tomography–CT

Positron emission tomography (PET) is an established imaging technique, most commonly used in oncology. PET utilizes radionuclides that decay by positron emission. Positron emission occurs when a proton-rich unstable isotope transforms protons from its nucleus into neutrons and positrons. PET is based on similar principles to other fields of scintigraphy whereby an isotope is attached to a biological compound to form a radiopharmaceutical, which is injected into the patient [56].

The most commonly used radiopharmaceutical in PET scanning is fluorodeoxyglucose (FDG) (2 deoxyglucose labeled with the positron-emitter fluorine-18). FDG is an analogue of glucose and therefore accumulates in areas of high glucose metabolism. Positrons emitted from the fluorine-18 in FDG collide with negatively charged electrons. The mass of an electron and positron is converted into two 511 keV photons, i.e. high-energy gamma rays, which are emitted in opposite directions to each other. This event is known as annihilation (Fig.5.4). The PET camera consists of a ring of detectors that register the annihilations. An area of high concentration of FDG will have a large number of annihilations and will be shown on the resulting image as a ‘hot spot’. Normal physiological uptake of FDG occurs in the brain (high level of glucose metabolism), myocardium, and in the renal collecting systems, ureters and bladder. Tracer (positron emitter) is injected into patient and accumulates in region of interest (e.g. high metabolism) [57].

The current roles of PET imaging may be summarized as follows, Oncology include tumor staging, assessment of tumor response to therapy, differentiate benign and malignant masses, e.g. solitary pulmonary nodule, and detect tumor recurrence. Cardiac: Non-invasive assessment of myocardial viability in patients with coronary artery disease. Central nervous system characterization of dementia disorders and localization of seizure focus in epilepsy [58].

As with other types of scintigraphy, a problem with PET is its non-specificity. Put another way, ‘hot spots’ on PET may have multiple causes, with false positive findings commonly encountered. The specificity of PET may be increased by the use of scanners that fuse PET with CT or MRI. PET– CT fusion imaging combines the functional and metabolic information of PET with the precise cross- sectional anatomy of CT (Fig. 5.5). Advantages of combining PET with CT include reduced incidence of false positive findings in primary tumor staging and increased accuracy of follow-up of malignancy during and following treatment.

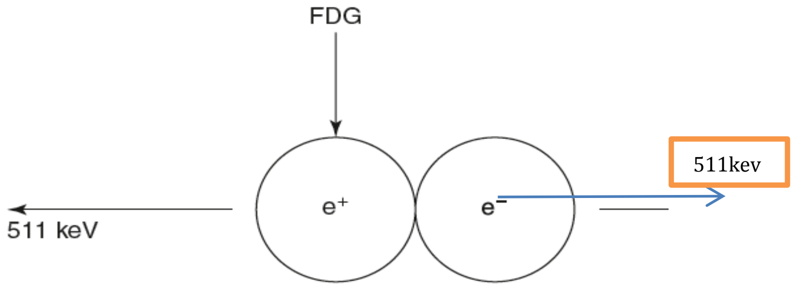

Figure 5.4: Annihilation. A positron (e+) emitted by an FDG molecule encounters an electron (e−). The two particles annihilate converting their mass into energy in the form of two 511 keV gamma rays, which are emitted in opposite directions [57].

PET–CT scanners are now widely available and have largely replaced stand-alone PET scanners in modern practice**.** At the time of writing, PET–MR scanners are also becoming available in research and tertiary institutions.

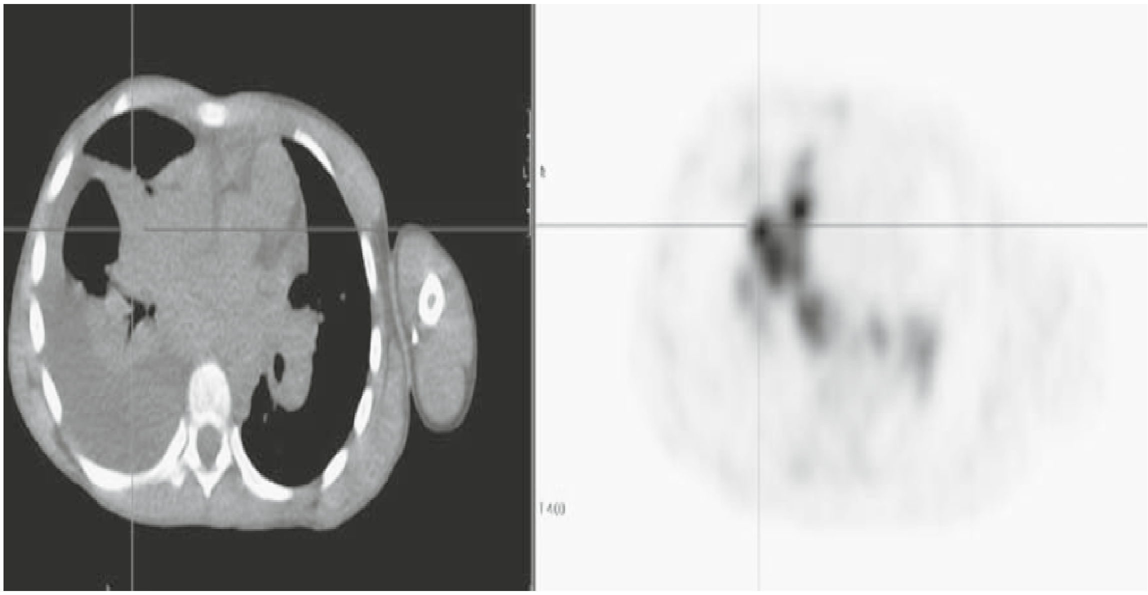

Figure 5.5: Positron emission tomography–CT (PET–CT): Hodgkin's lymphoma. CT image on the left shows neoplastic lymphadenopathy, collapsed lung and pleural effusion. Corresponding FDG-PET image on the right shows areas of increased activity corresponding to neoplastic lymphadenopathy. Collapsed lung and pleural effusion do not show increased activity, thus differentiating neoplastic from non-neoplastic tissue [56].

5.2 Applications of Neutron Activation Spectroscopy

Since the discovery in 1932, neutrons became a basis of many methods used not only in research, but also in industry and engineering. Among, the exceptional role in the modern nuclear engineering is played by the neutron activation spectroscopy, based on the interaction of neutron flux with atomic nuclei. Neutrons have many properties that make them ideal for certain types of application, especially concerning imaging and elemental traces detection techniques [58].

Neutron activation analysis (NAA) is a nuclear process used for determining the concentrations of elements in a vast amount of materials**.** NAA relies on excitation by neutrons so that the treated sample emits gamma-rays. It allows the precise identification and quantification of the elements, above all of the trace elements in the sample. NAA has applications in chemistry but also in other research fields, such as geology, archaeology, medicine, environmental monitoring and even in the forensic science.

Passing through matter neutrons interact with nuclei in several processes including the elastic and inelastic scattering, neutron capture, fission or particle emission from the nucleus. The inelastic scattering and neutron capture constitute base of the Neutron Activation Analysis techniques (NAA), which are widely used for the quantitative elemental concentrations determination. These two types of neutron interaction results in the nuclei excitation turning them into radioactive nuclides, which decay emitting gamma rays. Their energies are characteristic for each element, so that the measurement of these gamma rays intensities gives information on the elemental content of the irradiated object. Methods based on NAA have a big application potential since they provide an analysis of a large number of elements simultaneously and non-destructively. Moreover, they have a very low detection limits for many elements. Devices based on NAA are used widely in industry (eg., crude oil and coal deposits identification, water monitoring), medicine and homeland security [59].

NAA is an analytical technique based on the measurement of characteristic radiation from radionuclides formed directly or indirectly by neutron irradiation of the material of interest. In the last three decades, neutron activation analysis has been found to be extremely useful in the determination of trace and minor elements in many disciplines [60].

These include environmental analysis applications, nutritional and health related studies, geological as well as material sciences. Although there are several types of neutron sources (reactors, accelerators, and radio isotopic neutron emitters) one can use for NAA, nuclear reactors with their high fluxes of neutrons from uranium fission offer the highest available sensitivities for most elements.

In NAA, samples are activated by neutrons. During irradiation the naturally occurring stable isotopes of most elements that constitute the rock or mineral samples, biological materials are transformed into radioactive isotopes by neutron capture. Then the activated nucleus decays according to a characteristic half-life; some nuclides emit β particles only, but most nuclides emit gamma-quanta (gamma-photon), too, with specific energies. The quantity of radioactive nuclides is determined by measuring the intensity of the characteristic gamma-ray lines in the spectra. For these measurements a gamma-ray detector and special electronic equipment are necessary [61].

The method is based on conversion of stable atomic nuclei into radioactive nuclei by irradiation with neutrons and subsequent detection of the radiation emitted by the radioactive nuclei and its identification. The basic essentials required to carry out an analysis of samples by

NAA are a source of neutrons, instrumentation suitable for detecting gamma rays, and a detailed knowledge of the reactions that occur when neutrons interact with target nuclei.

The n-gamma reaction is the fundamental reaction for neutron activation analysis. For example, consider the following reaction:

$$^{58}Fe + {}^{1}n \rightarrow {}^{59}Fe + Beta\text{-} + \text{gamma rays}$$

^{58}Fe is a stable isotope of iron while ^{59}Fe is a radioactive isotope. The gamma rays emitted during the decay of the ^{59}Fe nucleus have energies of 142.4, 1099.2, and 1291.6 keV, and these gamma ray energies are characteristic for this nuclide.

Basically, the technique is quite simple. A sample is irradiated by slow neutrons and becomes radioactive. By measuring the $\beta+$, $\beta-$, and γ emissions, and the half-life of the radioactive sample, the elemental constituents of the sample and their relative concentrations can be determined. Industrial activation analysis is usually done with slow neutrons from a reactor, where the neutron flux can be as high as 5×10^{13} neutrons/cm^2/s, or with an accelerator with fast neutron fluxes of 10^{10} neutrons /cm^2/s. When activation analysis is compared with other analytical methods, such as gravimetric, colorimetric, spectrographic, or mass spectroscopy, its sensitivity is usually shown to be better by a factor of 10 than that of other methods [62]. Activation analysis is used extensively in such fields as geology, medicine, agriculture, electronics, metallurgy, criminology, and the petroleum industry.

The use of NAA techniques for medical applications was first reported in 1964 for measurement of sodium in the body. $Na^{23} + n \Rightarrow Na^{24}$ (γ 1.37; 2.75 MeV). Between 1968 and 1972, Chamberlain reported the measurement of body calcium and sodium in the body and described techniques for whole-body NAA and pulsed NAA.

$$\mathbf{^{48}Ca + n \Rightarrow {}^{49}Ca + \gamma\ (3.1\ MeV)}$$

Total body calcium by whole body neutron activation: new technique for study of bone disease. Cohn and Dombrowski reported the measurement of calcium, sodium chlorine, nitrogen, and phosphorus in the human body through in vivo NAA. Since then, NAA has been used for a variety of applications, such as the measurement of nitrogen, carbon and oxygen, cadmium, and manganese in the body and in trace element research to identify cancerous tissue [63].

NAA has been applied for determining many elements, usually trace elements, in the following fields and sample types:

- Biomedicine, animal and human tissues activable tracers, bile, blood and blood components, bone, brain cell components and other tissues, breast tissue, cancerous tissues, colon, dialysis fluids, drugs and medicines, eye, faeces, foetus, gallstones, hair, implant corrosion, kidney and kidney stones, snake venom, rat tissues (normal and diseased), teeth, dental enamel and dental fillings, thyroid, urine and urinary stones.
- Environmental science and related fields — aerosols, atmospheric particulates (size fractionated), dust, fossil fuels and their ashes, flue gas, animals, birds, insects, fish, aquatic and marine biota, seaweed, algae, lichens, mosses, plants, trees (leaves, needles, tree bark), soils, sediments and their leachates, sewage sludges, tobacco and tobacco smoke, surface and ground waters, volcanic gases.
- Geology and geochemistry — asbestos, bore hole samples, bulk coals and coal products, coal and oil shale components, crude oils, kerosene, petroleum, cosmo-chemical samples, cosmic dust, lunar samples, coral, diamonds, exploration and geochemistry, meteorites, ocean nodules, rocks, sediments, soils, glacial till, ores and separated minerals.
- Industrial products — alloys, catalysts, ceramics and refractory materials, coatings, electronic materials, fertilizers, fissile material detection and other safeguard materials, graphite, high purity and high-tech materials, integrated circuit packing materials, online, flow analysis, oil products and solvents, pharmaceutical products, plastics, process control applications, semiconductors, pure silicon and silicon processing, silicon dioxide, NAA irradiation vials, textile dyes, thin metal layers on various substrates.

In general, NAA is a versatile and non-labor intensive analytical technique. Liquids, solids, and gases can be analyzed by NAA. It is a multi-element technique in that many elements can be analyzed simultaneously in a given sample spectrum without changing or altering the apparatus as is necessary in atomic absorption, etc. Importantly, special sample preparations, such as digestion or extractions, are not required, and therefore the NAA method is non-destructive, i.e., the integrity of the sample is not changed in any manner by prechemistry or the addition of any foreign materials for irradiation [64].

Conclusion

- From this review work it is concluded that gamma spectroscopy techniques should be widely applied in Ethiopia in elemental analysis methods like Neutron Activation Analysis (NAA) in various fields such as geology, medicine, agriculture, electronics, metallurgy, criminology, environmental science, petroleum industry, and industrial products. This will enhance capacity in different sectors and there by contribute for the development of the country.
- In this paper a review of gamma ray spectroscopy is given with a particular emphasis and it is a very useful tool for the characterization molecules due to its higher detection selectivity, sensitivity and rapidity for the compound analysis compared to that of other spectroscopic analytical techniques.
- The three interactions of gamma-rays with matter are Photoelectric effect, Compton scatter and Pair production. In photoelectric effect all of the energy of the incoming photon is totally transferred to the atom but in Compton scatter an incoming photon is partially absorbed in an outer shell electron and Pair production process is a conversion of energy into matter and then matter back into energy.
- The most common (not the only) detectors in gamma spectroscopy systems are of thallium doped sodium iodide (NaI (Tl)), hyper pure germanium (HPGe) and CdZnTe (Cadmium zinc telluride). A pulse is produced for each gamma ray interacting in the detector and pulse is a short-term change in the voltage. The greater the energy deposited in the detector, the larger the pulse. Generally, the sensitivity of a HPGe system will be in direct proportion to the detector efficiency. Narrower peaks (better resolution) means a greater ability to distinguish gamma rays of similar energies HPGe detectors have much better resolution than NaI detectors. On a given spectrum, the peaks get broader as the energies get higher. In other words, peaks get broader as we move to the right.
- NAA plays a complementary role in materials analysis in an industrial analytical laboratory. There are applications where it is highly desirable, and may play the dominant role as the method of choice, e.g., bulk analysis of Si. Activation analysis is used extensively in such fields as geology, medicine, agriculture, electronics, metallurgy, criminology, and the petroleum industry.

Bibliography

[1] AN34: Experiments in Nuclear Science, 3rd Ed., EG & G Ortec. Experiment 1, Basic identifications in Electronic Measurement Systems, pp 1-7; Experiment 3, Gamma Spectroscopy Using NaI, pp 15-24; Linear and Logic Signals in EG & G Ortec NIM Instruments, pp159-160

[2] K. Siegbahn, *Alpha, Beta and Gamma-Ray Spectroscopy*, Vol. I, particularly Chapts. 5, 8A.

[3] F. Adams and R. Dams, ***Applied Gamma-Ray Spectroscopy*** (Pergamon Press, Oxford, 1970). Although older than Reference 1, this work provides a comprehensive coverage of gamma-ray spectroscopy. Information is available on NaI and germanium detectors and the accompanying instrumentation.

[4] D.W. Ball, *Field Guide to Spectroscopy (for EMW spectrum)*(SPIE Press, Bellingham, Washington, 2006).

[5] W. C. Roentgen: On a New Kind of Rays, December 28, 1895. (*Preliminary Communication)*

[6] de Hevesy GC. Marie Curie and her contemporaries. 1 Nucl Med 1984; 25: 118-31.

[7] Bull JWD. Neurology's debt to Becquerel. Br J Radiol 1972; 45: 881-90.

[8] R. Gunninlq J. E. Evans, and A. L. Prindle, “A Reevaluation of the Gamma-Ray Energies and Absolute Branching Intensities of 237U, 238’239*240’241Pu, and 241AmYLawrence Livermore Laboratory reportUCRL-52139 (1976).

[9] “Ctilbration Techniques for the Calorimetric Assay of Plutonium-Bearing Solids Applied to Nuclear Materials Control,” ANSI N15.22-1975 (American National Standards Institute, Inc., New York, 1975) and 1986 revision.

[10] J. H. Hubbell, “Photon Cross Sections, Attenuation Coefficients, and Energy Absorption Coefficients from 10 keV to 100 GeV,” National Bureau of Standards report NSRDS-NBS 29 (August 1969).

[11] . C. M. Ledmr and V. S. Shirley, E&., ***Table of Isotopes, 7th*** ed. (John Wiley 8C Sons, Inc., New York, 1978).

[12] T. Gozani, ***Active Nondestructive Assay of Nuclear Material, Principles and Applications,*** NUREG/CR-0602 (US Nuclear Regulatory Commission, Washington, DC, 1981).

[13] Beiser: Concepts of Modern Physics, pp 443, 471-473 (gamma decay)

[14] G. F. Knoll, ***Radiation Detection and Measurement*** (John Wiley& Sons, New York, 1979).

[15] Eisberg and Resnick, "Quantum Physics" Wiley, (1974).

[16] R. D. Evans, The ***Atomic Nucleus*** (McGraw-Hill Book Co., New York, 1955).

[17] R.D. Evans "Gamma Rays" Chap. 8e in "American Institute of Physics Handbook",
3rd Ed., McGraw–Hill, (1972).

[18] E. Storm and H. Israel, "Photon Cross Sections from 0.001 to 100 MeV for Elements
1 through 100," Los Alamos Scientific Laboratory report LA-3753 (1967).

[19] D.W. Preston & E.R. Dietz: The Art of Experimental Physics, Appendix B Counting and Sorting Particles: The Scintillation Counter, pp376-385 *general theory*

[20] Halliday: Introductory Nuclear Physics

[21] Serway, Moses and Moyer: Modern Physics, pp 431-432 (scintillator/photomultiplier), 389-392 (beta and gamma decay).

[22] G.F. Knoll, Radiation Detection and Measurement - 3rd edition (Chapters 2 and 10), John Wiley & Sons, 1999.

[23] K. Debertin, R.G. Helmer, Gamma- and X-ray Spectrometry with Semiconductor Detectors, North-Holland, 1988.

[24] M. Blaauw, M.J.J. Ammerlaan, S.J. Gelsema, Nucl. Intstr. and Meth. A 385 (1997) 330.

[25] J. B. Birks, The Theory and Practice of Scintillation Counting (Pergamon Press, Oxford, 1964).

[26] H. W. Cramer, C. Chasman, and K. W. Jones, "Effects Produced by Fast Neutron
Bombardment of Ge(Li) Gamma-Ray Detectors;' Nuclear Instruments and Methods 62, 173 (1968).

[27] R. H. Pehl, "Germanium Gamma-Ray Detectors," Physics Toalzy 30, 50 (Nov., 1977).

[28] Gamma-ray Spectrometry Center, Idaho National Laboratory, URL:
http://www.inl.gov/gammaray/catalogs/.

[29] J. M. Marler and V. L. Gelezunas, "Operational Characteristics of High-Purity
Germanium Photon Spectrometers Cooled by a Closed-Cycle Cryogenic Refrigerator," IEEE Transactions on Nuclear Science NS 20, 522 (1973).

[30] T. Prettyman, M.K. Smith, S.E. Soldner, "Design and Characterization of Cylindrical

CdZnTe Detectors with Coplanar Grids", Proceedings of SPIE (1999), Los Alamos National Laboratory document LA-UR-99-3117.

[31] Progress Report on IAEA/Technion - Israel Institute of Technology Research Contract No. 10400 "CdZnTe Arrays for Hand-Held Gamma Spectrometers, August 1999.

[32] R. H. Pehl, Germanium Gamma-Ray Detectors, Physics Today 30, 50 (Nov., 1977).

[33] Korun M, Martinčič R (1997) Measurement of the total- -to-peak ratio of a semiconductor gamma-ray detector.

[34] P. Siffert et al., "Cadmium Telluride Nuclear Radiation Detectors: IEEE Transactions on Nuclear Science NS 22, 211 (1975).

[35] U. Fano, "On the Theory of Ionization Yield of Radiation in Different Substances:' Physics Review 70, 44 (1946); "Ionization Yield of Radiation II The Fluctuations in the Number of Ions," Physics Reviw 72, 26 (1947).

[36] C. Fiorini et al., Position and Energy Resolution of a new gamma-ray Detector based on a single CsI(Tl) Scintillator coupled to a Silicon Drift Chamber Array, IEEE NuclearScience Symposium and Medical Imaging Conference,Conference Record, Toronto, 1998,63, 8-14.

[37] B.D. Milbrath, B.J. Choate, J.E. Fast, W.K. Hensley, R.T. Kouzes and J.E. Schweppe, Comparison of LaBr3:Ce and NaI (Tl) scintillators for radio-isotope identification devices, Nucl.Instr. Meth. Phys. Research,2007;572- 774.

[38] Kaplanis, S.N. Geometric, effective solid angles and intrinsic efficiencies of a 3£3 NaI(Tl) for isotopic and non-isotopic photon emission.
Int. J. Appl. Radiat. Is. 1982, 33, 127–135.

[39] Warner, N.R.; Christie, C.A.; Jackson, R.B.; Vengosh, A. Impacts of shale gas wastewater disposal on water quality in western Pennsylvania. Environ. Sci. Tech. 2013, 47, 11849–11857.

[40] Jodłowski P (2005) Gamma-ray spectrometry of environmental samples; radioactive nuclides in the ecosystem of the Gorce Mountains (Poland). PhD Thesis. AGH University of Science and Technology, Kraków (in Polish).

[41] F. Adams and R. Dams, Applied Gamma-Ray Spectrometry (Pergamon Press New York, 1975).

[42] Jodłowski P (2006) Self-absorption correction in gamma-ray spectrometry of environmental samples – an overview of methods and correction values obtained for the selected geometries. Nukleonika 51;S2:S21–S25

[43] U.S. Environmental Protection Agency (2007) SW-846 EPA Method 6020A rev. 1: Inductively Coupled Plasma-Mass Spectrometry.

[44] Jodłowski P (2005) Gamma-ray spectrometry of environmental samples; radioactive nuclides in the ecosystem of the Gorce Mountains (Poland). PhD Thesis. AGH University of Science and Technology, Kraków (in Polish)

[45] A. Shakhahiro, U. Sansone, Radionuclide activity measurements in environ- mental samples of water, soil and grass: CCRI(II)-S4 comparison report, Technical Supplement, vol. 46, 2009, p. 06004 CRI(II)-S4.

[46] Amaral, E. M., 2000. *Natural gamma radiation in air versus soil nature in Portugal*. International Radiation Protection Association, P-1a-12.

[47] Anastasiou, T., Tsertos, H., Christofides, S., Christodoulides, G., 2002**.** *Indoor radon concentration measurements in Cyprus using high-sensitivity portable detectors.* Preprint UCY–PHY–02/04 (submitted to Jour. of Env. Radioactivity).

[48] Hamby, D. M., Tynybekov, A. K., 2002. *Uranium, thorium and potassium in soils along the shore of lake Issyk-Kyol in the Kyrghyz Republic*. Environmental Monitoring and Assessment 73, 101-108.

[49] Basic Science of Nuclear Medicine, 2nd Ed., RP Parker, PHS Smith, DH Taylor (Churchill Livingstone, 1984)

[50] Harrison, R. (2012). In: Grupen, C. & Buvat, I. (Ed.), *Simulation of Medical Imaging Systems: Emission and Transmission Tomography*, Springer Berlin Heidelberg.

[51] C. Lang *et al*. (2014). Sub-millimeter nuclear medical imaging with high sensitivity in positron emission tomography using b+g coincidences, JINST 9 P01008. doi:10.1088/1748-0221/9/01/P01008.

[52] Donohoe KJ, Brown ML, Collier BD, et al. Procedure Guidelines for Skeletal Scintigraphy, version 3.0. Society of Nuclear Medicine and Molecular Imaging Practice Guidelines, 2003.

[53] Guidelines and Standards Committee of the ACR Commission on Nuclear Medicine in collaboration with the SPR. ACR-SPR Practice Guideline for the Performance of Adult and Pediatric Skeletal Scintigraphy (Bone Scan). American College of Radiology and Society of Pediatric Radiology, 2012.

[54] [58] [Das13] Dash A, Knapp Jr FF, Pillai MRA. (2013). 99Mo/99mTc separation: An assessment of technology options. *Nucl Med Biol* 40: 167.

[55] M. Goitein, *Radiation Oncology: A physicist'seye view*, Springer, New York, 2007.

[56] [Bat06] Bateman TM *et al*. (2006). Diagnostic accuracy of rest/stress ECG gated Rb-82 myocardial perfusion PET: comparison with ECG-gated Tc-99m sestamibi SPECT. *J Nucl Cardiol* 13: 24.

[57] Stevens Anthony, Development of PET in Western Europe, presented at EANM 2011.

[58] De Corte, F.,The k0 Standardization Method: A Move to the Optimization of NAA, Gent University; 1987.

[59] Alghem, L., Ramdhane ,M., S. Khaled, T. Akhal., The development and application of k0-standardization method of neutron activation analysis at Es-Salam research reactor, Nucl. Instr. and methods., 556; 2006, p386–390.

[60] Alghem Hamidatou, L., Ramdhane, M., Characterization of neutron spectrum at Es- Salam Research Reactor using Høgdahl convention and Westcott formalism for the k0-based neutron activation analysis, Journal of Radioanalytical and Nuclear volume 278 issue (3); 2008, p627-630.

[61] De Corte, F., Simonits, A., Bellemanns, F, Freitas, MC., Jovanovic, S, Smodis, B., Erdtmann G., Petri, H., De Wispelaere, A., Recent advances in the k0-standardization of neutron activation analysis: Extensions, applications, prospects. J Radioanal Nucl Chem volume 169; 1993, p125–158.

[62] HEYDORN, K., Validation of NAA Techniques, in Quality Assurance for Environmental Analyses (QUEVAUVILLER, Ph., MAIER E.A., GRIEPINK, B. Eds), Elsevier (1995) 89–110.

[63] BYRNE, A.R., KUČERA, J., "Role of the self-validation principle of NAA in the quality assurance of bioenvironmental studies and in the certification of reference materials", Proc. Int. Symp. Harmonisation of Health-related Environ. Measurements using Nucl. and Isotopic techniques (Hyderabad, 4–7 Nov. 1996), IAEA Vienna (1997) 223–238.

[64] INTERNATIONAL ATOMIC ENERGY AGENCY, Report of a Technical Committee Meeting, Vienna, 4–7 May, 1993, Use of Neutron Beams for Low and Medium Flux Research Reactors: Radiography and Materials Characterization, IAEA-TECDOC-837, Vienna (1995).

Declaration

This project is my original work, has not been presented for a degree in any other University and that all the sources of material used for the project have been dully acknowledged.

Name: Yohannes Teffera
Signature: ______________________________
Place and time of submission: Addis Ababa University, August 2018
This project has been submitted for examination with my approval as University advisor.
Name: Dr. Tilahun Tesfaye
Signature: _______________________________